UNITED STATES AIR FORCE

INSTITUTE OF TECHNOLOGY

AIR UNIVERSITY

RESIDENT INSTRUCTION DIVISION

SOME DYNAMIC RESPONSE CHARACTERISTICS
OF WEIGHTLESS MAN

THESIS

GAE 62 Charles E. Whitsett, Jr.
1st Lt USAF

WRIGHT-PATTERSON AIR FORCE BASE-OHIO

SOME DYNAMIC RESPONSE CHARACTERISTICS OF WEIGHTLESS MAN

THESIS

Presented to the Faculty of the School of Engineering of
the Air Force Institute of Technology
Air University
in Partial Fulfillment of the
Requirements for the Degree of
Master of Science

By

Charles Edward Whitsett, Jr., B.A.E.

First Lieutenant USAF

Graduate Aeronautical Engineering

August 1962

Preface

Space exploration and the problems associated with this exciting adventure have fascinated me for years. My search for a thesis topic in this area ended when 1st Lieutenant L. L. Bucciarelli introduced me to the subject of stabilization of man in space, a phase of space exploration whose theoretical aspects provided the challenge for which I had been looking. Capt. John C. Simons' introduction into some practical aspects further motivated me to study this phase of the Man-In-Space program. In particular, he expressed the requirement for more information bridging the gap between anthropometric data and man's dynamic response characteristics needed for engineering design. The study has proven to be immensely interesting and an education in the field of weightlessness.

This report is the result of my attempt to describe a mathematical model which would represent flexible, weightless man and his dynamic response characteristics in a zero gravity environment. While no closed form, general solutions are given for the more complex, non-linear dynamics problems, several idealized problems are investigated which have direct relation to the actual case. An attempt has been made to present this information in a form useful to both the human-factors specialist and the design engineer.

I would like to express my thanks to Capt. Simons of the Behavioral Sciences Laboratory, Aerospace Medical Research Laboratories, Wright-Patterson AFB, Ohio, and Lt. Bucciarelli, my thesis adviser, for their

sincere interest, suggestions, and guidance throughout this study. Also, my thanks to Technical Sergeants Harold Espensen and William Sears for conducting and serving as subjects in the zero-gravity experiments, to Mr. Charles E. Clauser for his suggestions on the math model, and to A/1C Paul Bunch for his assistance with some of the photographic work.

Finally, I would like to thank my wife, Evie, for her sacrifice, interest, and encouragement, and my daughter, Edie, for her frequent, but usually welcomed diversions.

Charles E. Whitsett, Jr.

Contents

Page

List of Figures

List of Tables

Abstract

A mathematical model is developed to approximate the mass distribution, center of mass, moments of inertia, and degrees of freedom of a human being by segmenting the body into 14 idealized masses. An analysis of the model reveals that the moments of inertia about the segment mass centers of the hands, feet, and forearms are negligible, when compared to the total body moments of inertia. However, the moment of inertia of the torso about its mass center is 10% to 35% of the total body moment of inertia. By neglecting the local moments of inertia of the smaller segments, a simplified method is achieved for calculating the moments of inertia and center of mass when the body posture changes. An investigation of some selected problems in thrust misalignment, maneuvering, free-body dynamics, stability of rotation, and torque application reveals their applicability in predicting analytically man's dynamic response characteristics in space. Preliminary experiments indicate that the torque which weightless man can exert by applying a sudden twist to a fixed handle varies as a half sine wave, and is approximately 67% of his maximum torque under normal gravity conditions.

GAE/Mech 62-7

SOME DYNAMIC RESPONSE CHARACTERISTICS OF WEIGHTLESS MAN

I. Introduction

Subject and Purpose

The subject of this study is the dynamic response characteristics of weightless, flexible man. The purpose is to develop a mathematical model to represent the human body, and to use this model to predict analytically man's mechanical behavior to some selected problems associated with weightlessness.

Subject Background

As space operations are extended, man will be required to perform supply, assembly, maintenance, and rescue missions while weightless. Man in space, floating free from his space vehicle will experience degrees of freedom never encountered on earth. While "situated in a state of imponderability" (as Petrov has described weightlessness, Ref 15), any force applied by or to man will result in translational and/or angular accelerations. For instance, the force of an ordinary sneeze is sufficient to tumble the average individual at a rate of 1/5 of a revolution per minute, if unrestrained (Ref 21).

If the free-floating space worker is to move from one point to another and be able to work when he gets there, he must be provided with

a personal propulsion and stabilization device (Refs 9, 17, and 18). Before such a system can be developed, however, certain design parameters must be established. These parameters are dependent upon the biomechanical properties of the human body. In order to bridge the gap between anthropometric data and the dynamic response characteristics needed for engineering design, a mathematical model is created. "Dynamic response characteristics" is used here to describe those mechanical effects which result when the human body is subjected to unbalanced forces. The model must then incorporate the biomechanical properties of the human body.

Many of these biomechanical properties change when the body shape changes. For instance, when man moves his appendages, his center of mass and moments of inertia change. The model must represent these variations also. Because of the complexity and flexibility of the human body, any analytical representation is only an approximation. This difficulty has led two bio-engineers (Ref 3) to describe man as a "non-symmetrical, fluid-filled sack of variable shape containing a large air bubble."

Scope

This study will be concerned with only those major dynamic effects which result when the human body is subjected to unbalanced forces, and not the resulting physiological and psychological effects.

A general survey is made of some selected free-body dynamics problems in which the kinematics of the body are simple, and where elasticity and damping of the body structure are neglected.

The experimental efforts are of preliminary nature and serve as guidelines for future study.

Development

The problem of describing or predicting the dynamic response characteristics of weightless man is approached in three phases:

1. Description and analysis of a mathematical model
2. Analytical prediction of some selected dynamic response characteristics
3. Comparison of some analytical results with experimental data

In accordance with the three phases of this study, Chapter II is devoted to the development of a mathematical model which will incorporate the biomechanical properties of man based on the anthropometry of any given subject. An analysis is made, using a model based on the U.S.A.F. "mean man," to determine the contribution of each of the various body segments to the total body moments of inertia. Based on this analysis, a simplified method of calculating the changes in moments of inertia and center of mass when the body posture changes is developed.

In Chapter III some selected dynamics problems are investigated which can be used to analytically predict some of the dynamic response characteristics of weightless man.

The results of the experimental validation phase of this study are described in Chapter IV.

Some concluding remarks about the objectives of the study and recommendations for future work are given in Chapter V.

II. The Mathematical Model

Weightless man will undergo transient angular and linear accelerations and decelerations as he is subjected to unbalanced external forces and moments. Internal forces and moments will be generated and reacted throughout the body when he moves his appendages. The mechanical response of the human body will depend upon the biomechanical properties of the body with respect to these special excitations. In order to develop a mathematical model which can be used to predict analytically how the human body will respond, these same biomechanical properties must be incorporated into the model.

The human body is, however, a very complex system of elastic masses whose relative positions change as the appendages are moved. To represent this system in exact analytical terms would require an infinite number of infinitesimal, rigid masses and an infinite number of degrees of freedom. "Degrees of freedom" refers to the minimum number of independent coordinates necessary to completely specify the position of a system in space. As larger and fewer masses are chosen, the representation becomes less complex but less accurate.

The problem of developing a mathematical model reduces to a determination of the optimum number and shape of the idealized masses or body segments on which the model's dynamic response characteristics are based. The optimum configuration of the model is determined on the basis of two criteria:

1. Simplicity - a minimum number of components of simple geometrical shape consistent with an accurate representation of the human body.

2. Adaptability - a model which can incorporate the biomechanical properties of any particular individual.

A simple, but reasonably accurate, model is desired to simplify analytical solutions to the related dynamics problems and make it easier to interpret physically the results. The degree of accuracy required depends upon the particular problem being investigated. For instance, when the flight characteristics of a fighter aircraft are computed, the pilot is assumed to be a point mass at some location in the fuselage since the dynamic characteristics of the man are negligible when compared to those of the aircraft. However, when a propulsion and stabilization device for the space worker is considered, then man's dynamic response characteristics become very important. The dynamic characteristics of the whole system will depend primarily on the man since he will be larger in size and mass than the propulsion and stabilization unit. Since a model for the latter application is desired for this study, a more refined model is developed than has been previously described (Ref 14, 18).

The propulsion and stabilization unit will probably be designed and built for each space worker; hence, it is desirable to know the dynamic response of each space worker. The mathematical model can be made to represent an individual by basing the model on the biomechanical properties of that individual.

Development of the Model

The most important biomechanical properties which will affect the dynamic response characteristics of man, and hence must be incorporated in the model, are:

1. the total mass and mass distribution
2. the location of the center of mass
3. the moments of inertia
4. the elasticity and damping of the body structure

Item numbers 2 and 3 vary as the body position changes; hence, this variation will also affect the response characteristics. Item number 4 becomes significant only when forces are applied very suddenly such as during an impact, and is not included in this study.

In order to develop the mathematical model, the human body is idealized based on the following assumptions:

1. The human body consists of a finite number of masses (or segments) and a finite number of degrees of freedom (hinge points).
2. The segments are rigid and homogeneous.
3. Each segment is represented by a geometric body which closely approximates the segment's shape, mass and center of mass, length, and average density.

The dynamic properties of these rigid, homogeneous, geometric bodies can be exactly determined.

Configuration of the Model. The mathematical model may be thought of as a system of rigid, honogeneous bodies of relatively simple geometric shape, hinged together in such a manner as to resemble the human body. For this study a 14 segment model is chosen. The division of the body into segments and the representative geometric bodies are shown in Figure 1. The hinge points are shown in Figure 2 and are defined as follows:

A. Neck - hinged only at the base of the neck (cervical)
B. Shoulder - hinged at the arm-shoulder socket

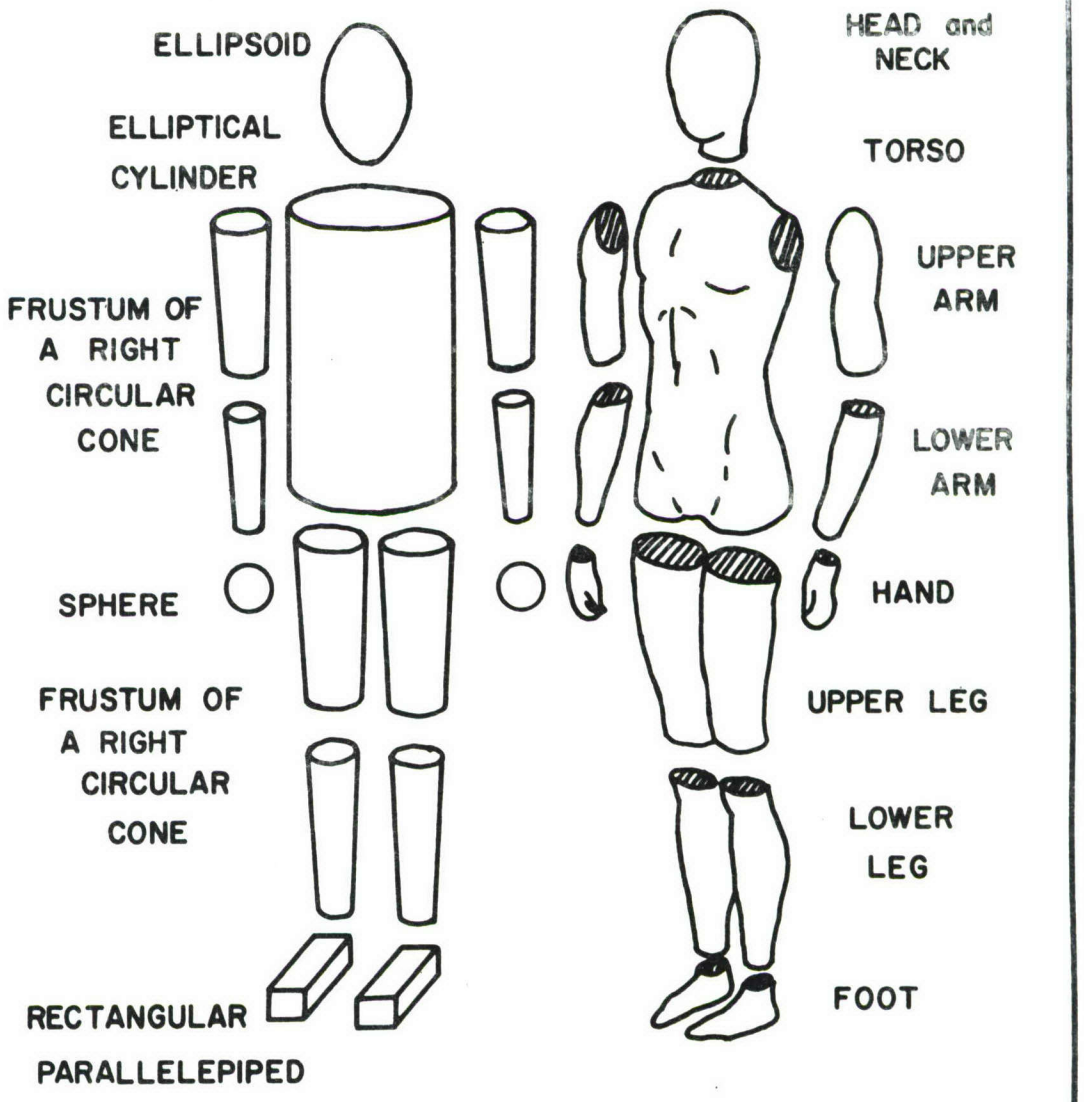

FIGURE I

SEGMENTED MAN AND MODEL

C. Elbow - hinged at the elbow joint

D. Hip - hinged at the leg-pelvis socket

E. Knee - hinged at the knee joint

The ankle and wrist joints are assumed rigid since their motion produces very slight variations in the total center of mass and moments of inertia.

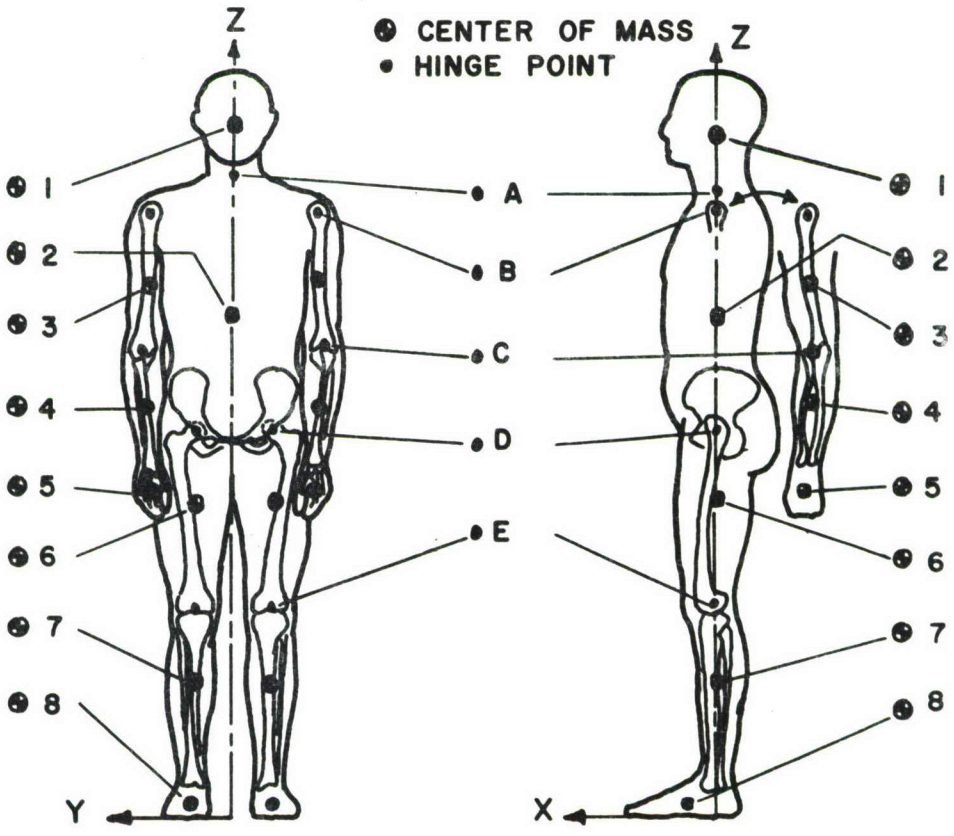

FIGURE 2

LOCATION OF CENTERS OF MASS AND HINGE POINTS OF THE HUMAN BODY

The model described has 24 degrees of freedom; six rigid body degrees of freedom plus 18 local degrees of freedom. The six rigid body degrees of freedom refer to the position and orientation of the body axis system. The other 18 degrees of freedom result from the nine hinge points, each

with two degrees of freedom. For instance, if a set of spherical coordinates is located at one shoulder hinge point, two angles must be specified to exactly locate the position of the upper arm.

The body axes system, shown in Figure 3, consists of a set of three orthognoal axes whose origin is always at the body center of mass and whose orientation remains fixed with respect to the axis system of the elliptical cylinder, as shown in Figure 4. The Z-axis remains parallel to the cylindrical axis, the x-axis perpendicular to the major and cylindrical axes, and the y-axis perpendicular to the minor and cylindrical axes. The positive directions and rotations are indicated in Figure 3.

A local body axis system is defined as a secondary orthogonal axis system located at the center of mass of each segment. Each is oriented in the same direction as the primary body axis system in the normal position defined in Figure 3 and remains fixed in position and direction with respect to that respective segment.

Biomechanical Properties. In order for the model to represent the dynamic response characteristics of man, certain biomechanical properties must be incorporated into the model. As stated earlier, these properties include mass, center of mass, average density, body dimensions, and moments of inertia. When these properties are used to define the properties of the geometric bodies which make up the model, the model will reflect the dynamic response characteristics of man. Some problems arise when the model is to represent a particular individual, since methods have not been developed for determining all these properties from living subjects. Fortunately, the most important property, body dimensions, can

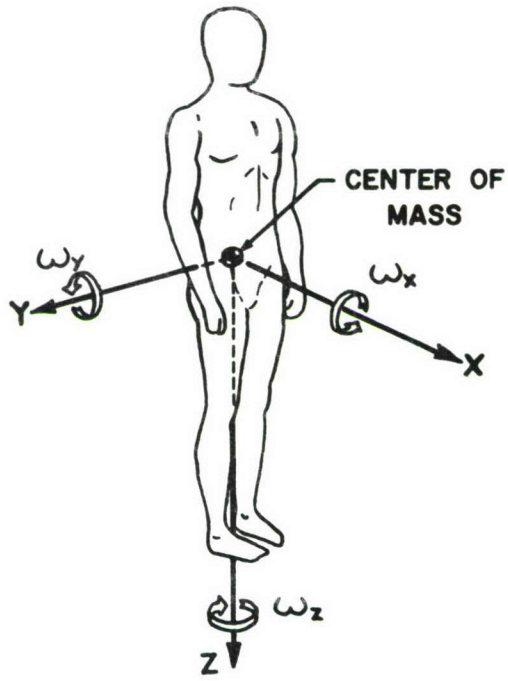

FIGURE 3
BODY AXIS SYSTEM

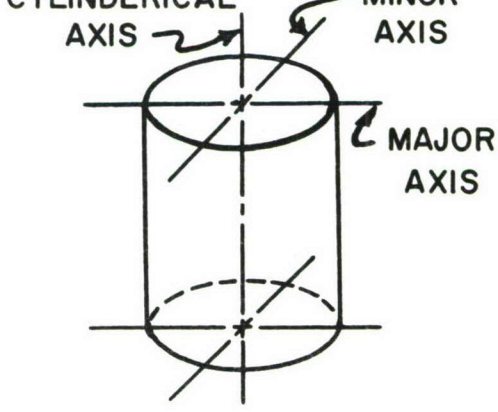

FIGURE 4
ELLIPTICAL CYLINDER

be readily attained. Hence for the model developed, only body measurement data (lengths of the segments, depths, breadths, and hinge point locations) is taken from the living subject. All other properties are estimated by the most reliable statistical methods available for various weight and body build groups. The methodology of obtaining the biomechanical properties of all the segments is described as follows.

The mass of all segments, except the head and torso, is estimated from the Regression Equations given by Barter (Ref 1:6) and are summarized in Table I. The head and torso equations are not given separately, therefore a method of determining the mass of these segments is developed herein.

Table I

Regression Equations for Computing the Mass (in Kg) of Body Segments (Ref 1:6)

Body Segment	Regression Equation
Both Upper Arms	0.08 x Total Body Weight - 1.3
Both Lower Arms	0.04 x Total Body Weight - 0.2
Both Hands	0.01 x Total Body Weight + 0.3
Both Upper Legs	0.18 x Total Body Weight + 1.5
Both Lower Legs	0.11 x Total Body Weight - 0.9
Both Feet	0.02 x Total Body Weight + 0.7

The center of mass location for the upper and lower arms and legs is taken directly from Dempster (Ref 4:194), and is given in Table D-I, Appendix D. For the other segments the center of mass is inherently at one-half the length and on the axis of symmetry.

The average density for all segments is also based on Dempster's study, and listed in Table D-I.

The lengths of the segments (defined as the vertical dimension of each segment as oriented in Figure 1) are based on the body measurement

data determined as indicated in Table II. The points and methods of measuring are given in Ref 12. Alternatively, the lengths may be taken directly from Ref 12 for a particular percentile group.

Table II

Segment Length from Anthropometry

Note: All heights are defined in Ref 12.

Segment	Length
Head	Stature - Cervical Height
Torso	Cervical Height - Penale Height
Upper Arm	Shoulder Height - Elbow Height
Lower Arm	Elbow Height - Wrist Height
Upper Leg	Penale Height - Kneecap Height +1.5 in.
Lower Leg	Kneecap Height - Lateral Malleolus Ht. -1.5 in.
Foot	Lateral Malleolus Height

The equations for calculating the mass moments of inertia for all the geometric bodies used in the model, except the frustum, are found in most mechanics textbooks (for example, Ref 5) and engineering handbooks (such as Ref 13). The equations for the mass moments of inertia of a frustum of a right circular cone are developed, in parametric form based on the center of mass location, in Appendix A. All equations are summarized in Table III.

The other basic dimensions required for the moment of inertia equations (such as the diameter, major axis, and minor axis) depend upon the particular segment. Their determination is included with the following general discussion of the geometric bodies chosen to represent each particular segment of the human body.

1. Head, Hand, and Foot. The motion of the neck is small in comparison to that of the head. Hence, the neck is considered to be

Table III

Formulae for Calculating Local Moments of Inertia of the Segments

Segment	Moments of Inertia		
	$I_{x_{c.g.}}$	$I_{y_{c.g.}}$	$I_{z_{c.g.}}$
Head	$\frac{1}{5} m (a^2 + b^2)$	$I_{x_{c.g.}}$	$\frac{2}{5} m a^2$
Torso	$\frac{1}{12} m (3a^2 + \ell^2)$	$\frac{1}{12} m (3b^2 + \ell^2)$	$\frac{1}{4} m (a^2 + b^2)$
Upper/Lower Arms & Legs	$m \left[A \left(\frac{m}{\delta \ell} \right) + B \ell^2 \right]$	$I_{x_{c.g.}}$	$2 \frac{m^2}{\delta \ell} A$
Hand	$\frac{2}{5} m \left(\frac{d}{2} \right)^2$	$I_{x_{c.g.}}$	$I_{x_{c.g.}}$
Foot	$\frac{1}{6} m \ell^2$	$\frac{1}{12} m (c^2 + \ell^2)$	$I_{y_{c.g.}}$

rigidly attached to the head. The head-neck combination is then represented by an ellipsoid of revolution. The major axis 2a is equal to the length dimension given in Table II. The minor axis 2b is found from

$$2b = \frac{\text{head circumference}}{\pi} \tag{1}$$

since the cross-section is circular.

The mass "m" is given by

$$m = \frac{4}{3} \delta \pi a b^2 \tag{2}$$

where δ is the average density of the head.

The mass of the hand is very small in comparison to the whole body (about 0.7%) and even though its shape varies considerably, the effect of this variation is negligible. Hence, the hand is greatly simplified and represented by a sphere. From

$$m = \frac{4}{3} \delta \pi \left(\frac{d^3}{8} \right) \tag{3}$$

we have

$$\text{diameter } d = 2\left(\frac{3m}{48\pi}\right)^{1/3} \tag{4}$$

The mass of the foot is quite small in comparison to the whole body (about 1.5%), hence it too is greatly simplified. The foot is represented by a rectangular parallelepiped whose height and width equals the length dimension for the foot given in Table II. The depth is equal to the instep length "c" (Ref 12).

2. Torso. The torso makes up approximately 48.5% of the total body mass. Consequently, its biomechanical properties will have a significant effect on the total body response.

An elliptical cylinder is chosen to represent the torso. The dimensions of the ellipse of the cross-section are given by:

Major axis (a) - Equal to the average of the body breadth measured at the chest, waist, and hips.

Minor axis (b) - Equal to the average of the body depth measured at the chest, waist, and hips.

In order to further substantiate the choice of an elliptical cylinder to represent the torso, a more detailed study was made to compare the average cross-sectional area of the human body to that of an ellipse based on the average breadth and depth.

Full scale cross-sectional area projections of the torso of a living subject of average build were provided by the Anthropology Section, Behavioral Sciences Laboratory, 6570th Aerospace Medical Research Laboratories. These were obtained by sterophotogrammetry (a photographic method of making contour maps of the human body). The cross-sectional areas at the chest, waist, and hip were measured with a planimeter. The average

area for subject number 35 was found to be 107.7 square inches. The breadth and depth were measured at the corresponding levels and averaged. The area of the representative ellipse was found to be 106.0 square inches from

$$\text{Area of ellipse} = \pi ab \tag{5}$$

where

$$a = \tfrac{1}{2} \text{ average breadth} \tag{6}$$

$$b = \tfrac{1}{2} \text{ average depth} \tag{7}$$

Of course the comparison for just one subject does not in itself justify the assumption that the torso can be represented by an elliptical cylinder; it does indicate that this is a reasonable approach.

3. Limbs. A frustum of a right circular cone is chosen to represent the upper and lower arms and legs because its center of mass can be made to coincide with that of the segment it represents. Parametric equations for moments of inertia are developed in Appendix A which are independent of all segment dimensions except length (given in Table II). A sample calculation is also given in Appendix A which illustrates the use of the parametric equations. Since there is no anthropometric data which coincides well with the height of the knee joint, this dimension is estimated by substracting 1.5 inches from the kneecap height.

4. Hinge points. The hinge points are assumed to be on the center line of the segments and are defined in Table IV.

Analysis of the Model

Since the center of mass and moments of inertia depend upon the position of the body segments, an analysis based on only one position is likely

Table IV

Location of Hinge Points from Anthropometry

Note: All measurements are defined in Ref 12.

Hinge Point	Coordinates*	
	Y	Z
Neck	o	Cervical Height
Shoulder	± 1/2 Biacromial Diameter	Shoulder Height
Elbow	± 1/2 Biacromial Diameter	Elbow Height
Hip	± 1/4 Hip Breadth	Penale Height
Knee	± 1/4 Hip Breadth	Kneecap Ht. - 1.5 in.

* All X coordinates are zero

to lead to some false conclusions. This section presents an analysis of the proposed mathematical model in two quite different positions.

Numerical Values. Numerical values of the biomechanical properties of the model are determined for the Air Force "mean man" (height 69.11 inches, weight 163.66 pounds) as described in Anthropometry of Flying Personnel-1950 (Ref 12). The mass, average density, length, and center of mass location of each segment are given in Table D-I. From this data the coordinates of the hinge points and segment centers of mass as defined in Figure 2 are determined and presented in Table D-II. Note that the origin of the coordinate system in Figure 2 is shifted to floor level. The coordinates in Table D-II are given in terms of this transposed coordinate system since all heights in Reference 12 are based on distance from the floor. From the data in Tables D-I and D-II and the formulae in Table III, the local moments of inertia are calculated and given in

Table D-III. The moments of inertia of each segment about the body axes are found from the parallel axis transfer equation

$$I = I_{c.g.} + md^2 \qquad (8)$$

where $I_{c.g.}$ is the local moment of inertia, "m" is the mass of the segment, and "d" is the distance between the body axis and a parallel axis through the center of mass of the segment. These values are given in Table D-III also.

Analysis. The dynamics of a rotating body in space depends primarily upon two factors: the center of mass location of the whole body; and the moments of inertia of the whole body about axes through the body center of mass.

The variation of the center of mass of the human body has been studied extensively (Ref 11) and can be accurately predicted for a given body position without too much difficulty. The center of mass of the model is found to lie 39.09 inches from the floor or 56.6% of the body length. This falls within the 55 to 57.4% range determined experimentally by Dempster (Ref 4) and agrees closely with an average of 55.6% measured by Swearingen (Ref 20) on five living subjects.

Predicting the moments of inertia is somewhat more involved and likely to be less accurate. Therefore an analysis is made of the mathematical model to determine:

1. which segments have the greatest effect on the total moment of inertia
2. the effect of approximation errors due to representing the segments by geometrical bodies
3. and which segments can be further simplified without a significant loss in accuracy.

The first position (position "a", Figure 5) considered is the normal position, standing erect with arms at the sides. For the second position (position "b", Figure 5) the arms and legs are drawn up close to the torso to give a near-minimum moment of inertia about the x- and y-axes. The moments of inertia for position "b" are calculated in much the same way as for position "a" and presented in Table D-III. It is noted that for this new position, the center of mass moves 7.0 inches towards the head along the z-axis and 1.9 inches forward along the x-axis.

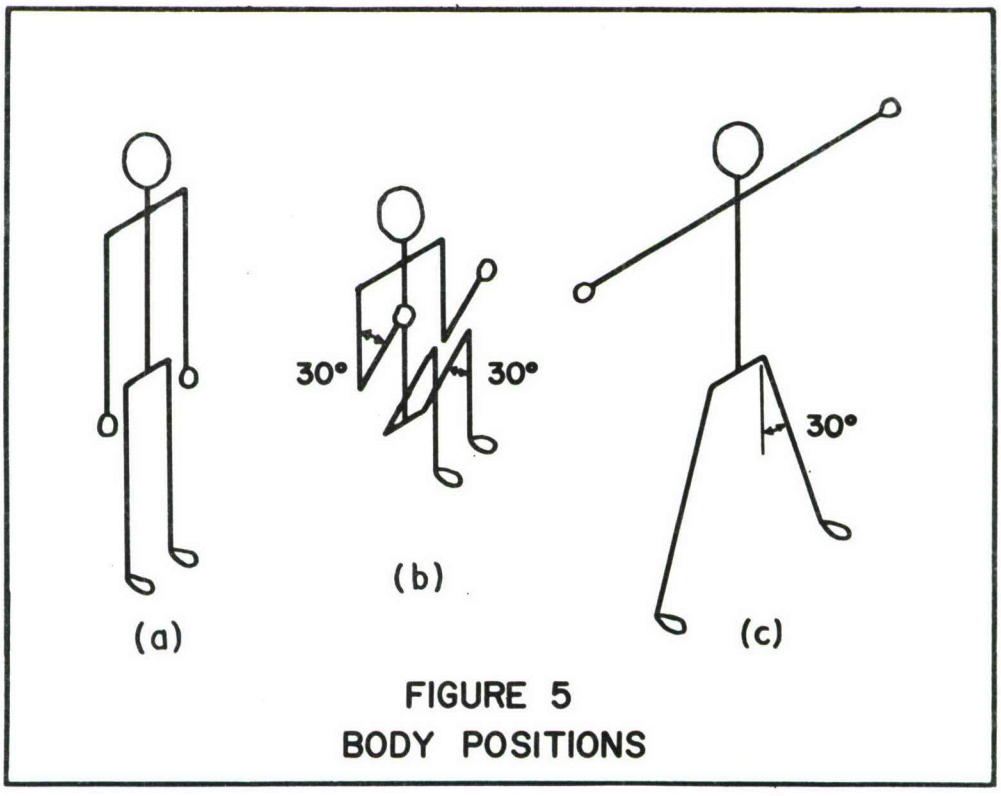

FIGURE 5
BODY POSITIONS

The moment of inertia of the whole body about a given axis is given by the sum of the moments of inertia of all segments about that axis. The moment of inertia of each segment as given by Eq 8 consists of two parts which are defined as follows:

Local Term $I_{c.g.}$: The moment of inertia of the segment about an axis through its center of mass parallel to the given axis

Transfer Term $m d^2$: A quantity given by the product of the mass of the segment times the square of the perpendicular distance between the two parallel axes.

Since the local terms are the most tedious to compute, it is of interest to see what contributions they make toward the total moment of inertia. In Figure 6 a comparison is made between the local and transfer terms for the two positions. Since these quantities are nearly the same about the x- and y-axes, the x-axis is not indicated.

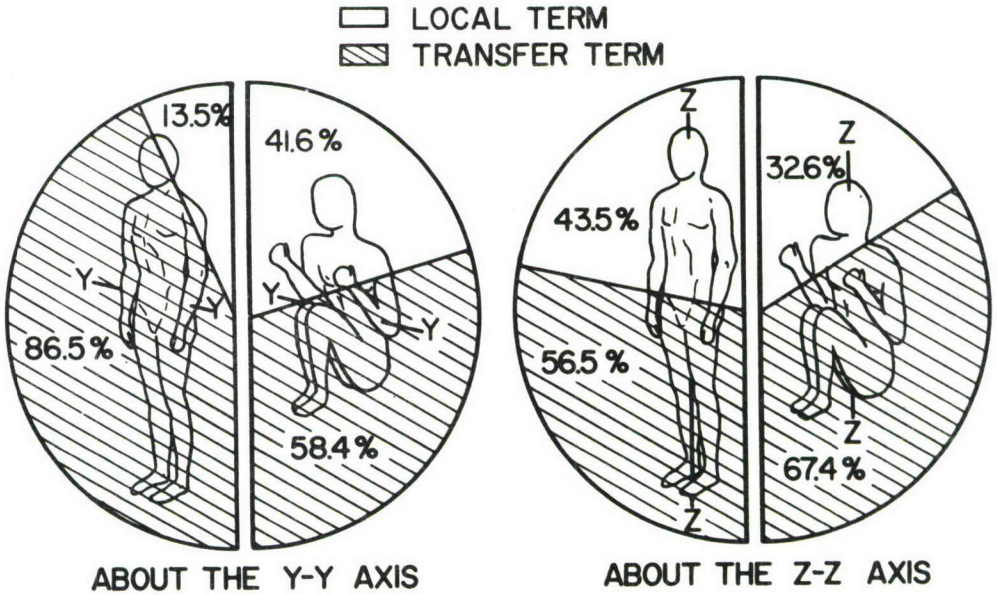

FIGURE 6
COMPARISON OF LOCAL TO TRANSFER MOMENT OF INERTIA TERMS
(EXPRESSED AS A PER CENT OF THE TOTAL MOMENT OF INERTIA)

Next, it is of interest to see what contribution each segment makes toward the total moment of inertia and what effects the local and transfer terms have on this quantity. This information is presented graphically in Figures 7 and 8.

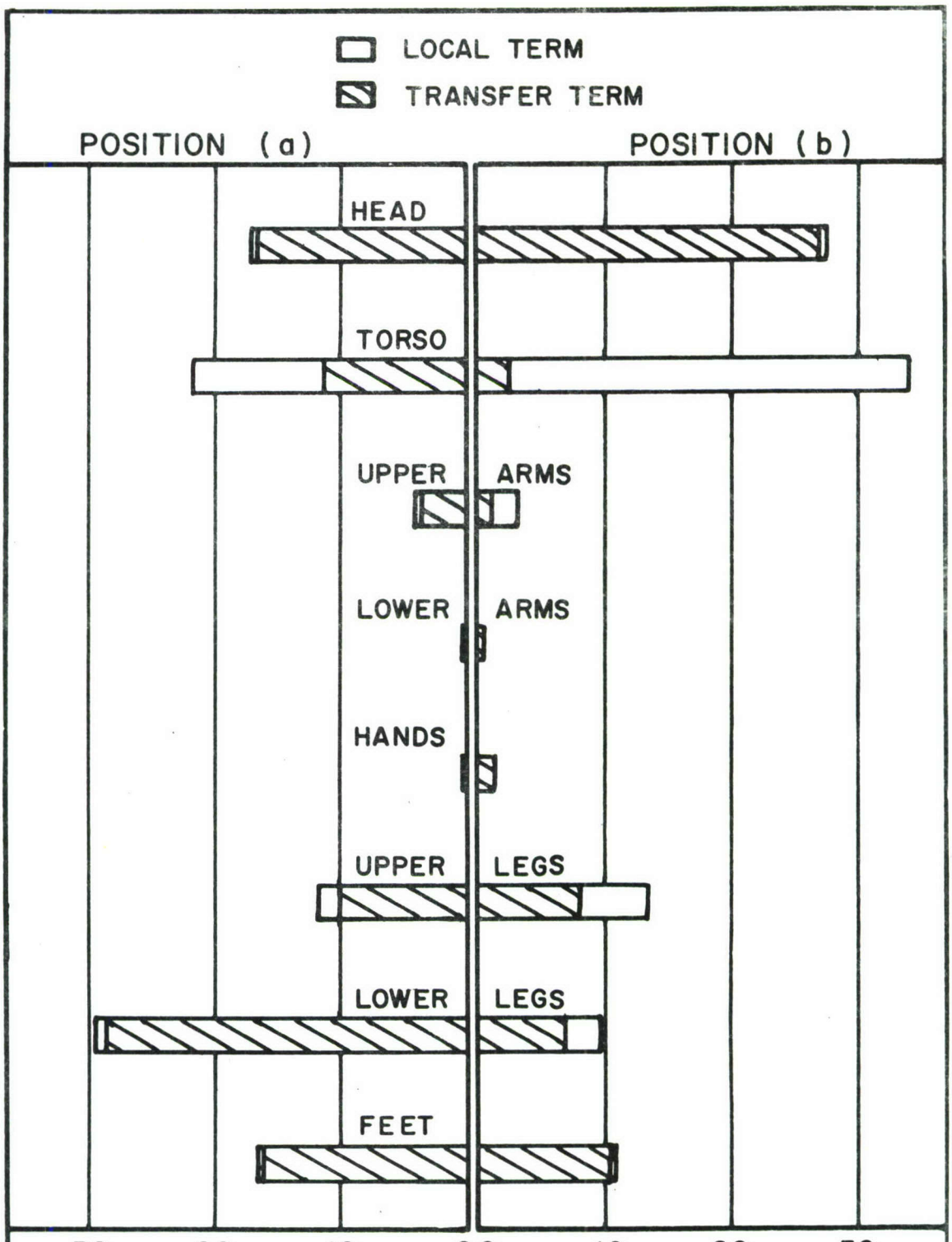

FIGURE 7

PER CENT OF TOTAL MOMENT OF INERTIA ABOUT THE Y-Y AXIS FOR EACH SEGMENT

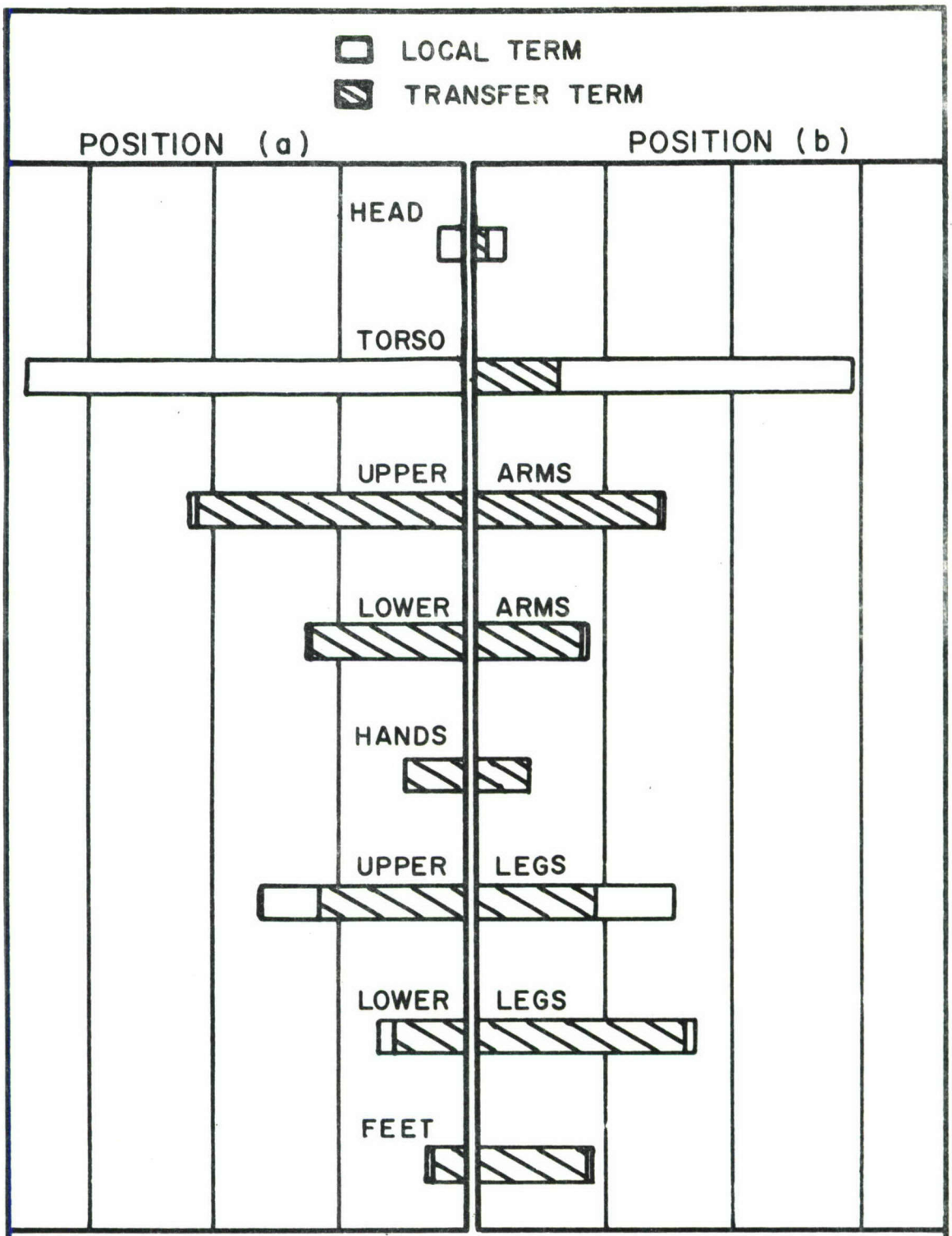

FIGURE 8

PER CENT OF TOTAL MOMENT OF INERTIA ABOUT THE Z-Z AXIS FOR EACH SEGMENT

Conclusions. A close look at Figures 6, 7, and 8 reveals some important information. In general the local moment of inertia terms can not be neglected, particularly about the z-axis. However, it can be seen that the contribution of the local term for several segments is zero or negligible. Hence, it can be concluded that it is unnecessary to compute the local moment of inertia for the hands, lower arms, and feet since their sum is less than the errors due to simplifying the human body. It can be further concluded that the geometric representation for the upper arms, upper and lower legs, and head need not be too accurate. For instance, a 33% variation in the moment of inertia of the upper arm would change the total moment of inertia (for position "a") about the x-axis only $\pm$ 0.1%. The total moment of inertia of the torso must be computed with much more care since it may contribute 10% to 35% of the total moment of inertia depending on the axis and position.

Simplified Approach. Based on the above conclusions, a simplified method is developed for computing the moments of inertia for various body positions. Starting with the moments of inertia for position "a" computed above as initial conditions $\left(I_{x_o}, I_{y_o}, I_{z_o}\right)$, this method yields the moments of inertia for any other position $\left(I_x, I_y, I_z\right)$ by taking into account only the changes in the transfer terms and the relative position of the body axis system. This approach greatly simplifies the mathematics, and although it neglects the changes in the local terms, there is only a slight reduction in accuracy.

The moment of inertia of the model (consisting of "p" masses or segments) about the x-axis for position "a" is given by

$$I_{x_o} = \sum_{i=1}^{p} I_{x_{io_{c.g.}}} + \sum_{i=1}^{p} m_i \left(y_{io}^2 + z_{io}^2\right) \qquad (9)$$

When the body position changes, the moment of inertia about the same axis is given by

$$I'_{x_o} = \sum_{i=1}^{p} I_{xi_{c.g.}} + \sum_{i=1}^{p} m_i \left(y_i^2 + z_i^2 \right) \tag{10}$$

To find the moment of inertia about a parallel axis through the center of mass for this new position, the Parallel Axis Transfer Theorem is used

$$I'_{x_o} = I_x + M\left(\bar{y}^2 + \bar{z}^2 \right) \tag{11}$$

now

$$I_x + M\left(\bar{y}^2 + \bar{z}^2 \right) = \sum_{i=1}^{p} I_{xi_{c.g.}} + \sum_{i=1}^{p} m_i \left(y_i^2 + z_i^2 \right) \tag{12}$$

Subtracting Eq 9 from Eq 12

$$I_x + M\left(\bar{y}^2 + \bar{z}^2 \right) - I_{x_o} = \sum_{i=1}^{p} I_{xi_{c.g.}} + \sum_{i=1}^{p} m_i \left(y_i^2 + z_i^2 \right) - \sum_{i=1}^{p} I_{xi_{o\,c.g.}} - \sum_{i=1}^{p} m_i \left(y_{io}^2 + z_{io}^2 \right) \tag{13}$$

Assuming the local terms do not change

$$\sum_{i=1}^{p} I_{xi_{c.g.}} = \sum_{i=1}^{p} I_{xi_{o\,c.g.}} \tag{14}$$

and Eq 13 becomes

$$I_x = I_{x_o} - \sum_{i=1}^{p} m_i \left\{ \left(y_{io}^2 + z_{io}^2 \right) - \left(y_i^2 + z_i^2 \right) \right\} - M\left(\bar{y}^2 + \bar{z}^2 \right) \tag{15}$$

Now if only "n" masses change position, the coordinates of the "p-n" masses will remain the same and will cancel out. Then

$$I_x = I_{x_o} - \sum_{i=1}^{n} m_i \left\{ \left(y_{io}^2 + z_{io}^2 \right) - \left(y_i^2 + z_i^2 \right) \right\} - M\left(\bar{y}^2 + \bar{z}^2 \right) \tag{16}$$

In a similar manner the equations for the moments and products of inertia about the other axes are found to be (Ref 8)

$$I_y = I_{y_o} - \sum_{i=1}^{n} m_i \left\{ \left(x_{io}^2 + z_{io}^2 \right) - \left(x_i^2 + z_i^2 \right) \right\} - M\left(\bar{x}^2 + \bar{z}^2 \right) \tag{17}$$

$$I_z = I_{z_o} - \sum_{i=1}^{n} m_i \left\{ \left(x_{io}^2 + y_{io}^2 \right) - \left(x_i^2 + y_i^2 \right) \right\} - M\left(\bar{x}^2 + \bar{y}^2 \right) \tag{18}$$

$$I_{xy} = \sum_{i=1}^{n} m_i \left\{ \left(x_i y_i \right) - \left(x_{io} y_{io} \right) \right\} - M\left(\bar{x}\,\bar{y} \right) \tag{19}$$

$$I_{yz} = \sum_{i=1}^{n} m_i \left\{ (y_i z_i) - (y_{io} z_{io}) \right\} - M(\bar{y}\bar{z}) \tag{20}$$

$$I_{zx} = \sum_{i=1}^{n} m_i \left\{ (z_i x_i) - (z_{io} x_{io}) \right\} - M(\bar{z}\bar{x}) \tag{21}$$

where

$$\bar{x} = \frac{1}{M} \sum_{i=1}^{n} m_i (x_i - x_{io}) \tag{22}$$

$$\bar{y} = \frac{1}{M} \sum_{i=1}^{n} m_i (y_i - y_{io}) \tag{23}$$

$$\bar{z} = \frac{1}{M} \sum_{i=1}^{n} m_i (z_i - z_{io}) \tag{24}$$

m_i ≡ mass of the ith segment

$x_i\, y_i\, z_i$ ≡ coordinates of the center of mass of the ith segment after some change

$x_{io}\, y_{io}\, z_{io}$ ≡ coordinates of the centers of mass of the ith segment before some change

M ≡ total mass

and "n" is the number of segments which change positions from the initial conditions. For instances, if one arm is raised from position "a", the center of mass of the upper and lower arm, and hand will change. Three segments are involved so $n = 3$ and m_1 might refer to the mass of the upper arm, m_2 to the mass of the lower arm, and m_3 to the mass of the hand.

It is pointed out that Eqs 22, 23, and 24 are exact and will always yield the coordinates of the new center of mass with respect to the center of mass location for position "a".

Up to this point, nothing has been said about products of inertia (I_{xy}, I_{yz}, I_{zx}). It should be realized that while in position "a"

the body axis system coincides with the principal axes of inertia and there are no products of inertia, this will not be true in general. Principal axes of inertia are defined as a set of orthogonal axes about which the products of inertia are zero. In fact, in position "b" the principal axes are tilted forward (rotated about the y-axis in the negative direction) approximately 8° from the body axes. Therefore, a product of inertia I_{zx} exists.

From Eqs 16, 17, and 18 the moments of inertia of the model are computed for positions "b" and "c". These results are compared with exact results taking the local terms into account in Table V.

Table V

Comparison of Moments of Inertia from Exact and Approximate Methods

	Moments of Inertia (Slug-ft^2)					
	I_x for Position		I_y for Position		I_z for Position	
	"b"	"c"	"b"	"c"	"b"	"c"
Exact Method	3.0496	12.225	2.9445	8.8430	1.0004	3.6210
Approximate Method	3.0845	12.225	2.9445	8.7917	0.9668	3.5356
Error	+1.14%	0.00%	0.00%	-0.58%	-3.36%	-2.36%

It should be noted that the approximate method yields exact results for I_x, position "c", and I_y, position "b". This occurs because there is no change in the local moment of inertia terms $I_{x_{c.g.}}$ for position "c" and $I_{y_{c.g.}}$ for position "b".

III. Analytical Results

The problems of dynamics facing the weightless man are many and varied. "Free-floating man is indeed an intimate man-machine unit, a single vehicle-driver component capable of fantastic motion behavior." (Ref 19) In this chapter several important problems are reviewed and analytical results are presented.

Thrust Misalignment

In order for a man (initially at rest) to move between two points in space, some external force must be applied. If translation is to take place without rotation, the resultant force must act through the man's center of mass. Since man is not a rigid body, flexing and bending the various appendages will cause the center of mass to change position with respect to the body. Therefore, it is unlikely that any single force device would act through the center of mass. The case of a single force device rigidly attached to the space worker so that a constant force is applied, not through the center of mass provides an interesting space dynamics problem. It has practical application to any propulsion and stabilization device since thrust misalignment might occur during a malfunction of the system.

Consider a thrust misalignment which produces a constant moment about one of the principal moment of inertia axes. If $I_x = I_y$ and the moment is applied about the y-axis, the resulting motion will be a spin about the y-axis and the center of mass will move in the plane of the x-z axes. Proof of this statement and complete derivation of the equations of motion are given in Appendix B. Even for this restricted

two-dimensional problem, a closed form solution could not be achieved. However, the equations of motion were non-dimensionalized and by applying the Runge-Kutta Method (Ref 16) a machine solution was achieved on the AFIT IBM 1620 Digital Computer. A non-dimensional plot of the velocities is given in Figure B-1 and the trajectory in Figure B-2.

It is interesting to note that for this special case of plane motion, the trajectory always approaches a straight line which is inclined 45° to the original heading. While the angular velocity increases as long as the misaligned thrust is applied, the linear velocity of the center of mass approaches a limit as can be seen in Figure B-1.

As an example, if the AF "mean man" is subjected to a 10-pound thrust misaligned 7.0 inches along the z-axis, in the direction of the x-axis, a constant magnitude moment of 70 in-lbs is applied about the y-axis. When the values of moments of inertia for position "b" are taken as principal moments of inertia, a solution to this problem (see the example problem at the end of Appendix B) indicates that in 5 seconds, the man will be accelerated to an instantaneous angular velocity of 96 rpm; he will have completed four revolutions, and reached a linear velocity of 1.6 ft/sec. After 10 seconds, he will have made almost 16 revolutions, and will be rotating at a rate of 191 rpm while moving at a rate of 1.7 ft/sec.

Maneuvering

A problem somewhat similar to the misaligned thrust problem is controlled rotation or maneuvering. The space worker will be equipped with a propulsion and stabilization unit to maneuver around his or other space

vehicles. The question arises, is there an optimum way to perform a particular maneuver?

In this section a very simplified problem is analyzed with the objective of showing that there is a considerable variation in the fuel required to execute a given maneuver. The optimum condition is achieved when the maneuver is completed with minimum fuel consumption.

Consider the following hypothetical problem. The space worker is moving with a constant initial velocity V_o (relative to the space vehicle), and he desires to make a 90^o change in his flight path. How does he direct his thrust (thrust vector) such that after a period of time T, he is moving at the same rate V_o perpendicular to the original heading, and a minimum amount of fuel is consumed?

Three Thrust Programs. Three thrust programs are analyzed based on the following assumptions:

1. The man (including the maneuvering unit) is a mass particle.

2. The period "T" of thrust application is small so that the mass "m" of the system is considered constant.

These assumptions reduce the problem to one of particle dynamics and neglect problems associated with the orientation of the man and how the particular thrust program is achieved. In all three problems the same thrust is applied although the length of time and direction vary. Since fuel consumption will depend solely upon the time applied for a constant magnitude thrust, the problem becomes one of determining the minimum thrusting time "T".

Case I. First consider the case in which the thrust F_o is applied in direct opposition to the initial motion until this motion ceases.

Then F_o is applied perpendicular to the original flight direction until a speed V_o is reached. From Newton's Equation

$$F = \frac{d(mv)}{dt} \tag{25}$$

and integrating with respect to time ($F = -F_o$)

$$-F_o t = mv + C \tag{26}$$

Applying the initial conditions $t = 0$, $V = V_o$

$$t = \frac{m}{F_o}(V_o - V) \tag{27}$$

Now at $t = t_1$, $V = 0$, so that the time to stop is t_1

$$t_1 = \frac{mV_o}{F_o} \tag{28}$$

By the same approach, the time to accelerate to V_o again is

$$t_2 = \frac{mV_o}{F_o} \tag{29}$$

therefore, the total thrusting time T is given by

$$T = t_1 + t_2 = \frac{2mV_o}{F_o} \tag{30}$$

If the initial velocity is in the x-direction and the final velocity is in the y-direction, the velocity components V_x and V_y will vary as shown in Figure 9, for Case I. While no values are shown for the plots in Figure 9, all are drawn to the same scale so that the results may be compared.

Case II. Suppose the decelerating force F_o is applied at a 45° angle in opposition to the initial motion so that one component of the force ($F_x = -0.707F_o$) acts in direct opposition to the original motion. Then the other component ($F_y = 0.707F_o$) will act normal to the initial flight path. Writing Newton's Equation in component form

$$F_x = \frac{d(mV_x)}{dt} \tag{31}$$

and integrating with respect to time ($F_x = -0.707F_o$)

$$-0.707F_o t = mV_x + C \tag{32}$$

Applying the initial conditions at $t = 0$, $V_x = V_o$

$$t = \frac{m}{0.707 F_o}\left(V_o - V_x\right) \tag{33}$$

Now at $t = t_1$, $V_x = 0$, the time to stop is

$$t_1 = 1.414 \frac{m V_o}{F_o} \tag{34}$$

By a similar approach

$$t_2 = 1.414 \frac{m V_o}{F_o} \tag{35}$$

Now F_x and F_y are applied simultaneously so that the complete maneuver is completed during time t_1, or

$$t_1 = t_2 = T \tag{36}$$

The variations of V_x and V_y are shown in Figure 9.

Case III. Consider now a case in which the thrust is applied normal to the flight path until the man has completed a 90^o turn. Then the thrust F_o will be equal to the centrifugal force or

$$F_o = \frac{m V_o^2}{R} \tag{37}$$

where R is the radius of curvature. Since there is no force applied tangent to the flight path, V_o remains constant and the flight path is an arc of a circle of radius R. The arc will be one-fourth of a circle. The time to cover this distance is given by

$$t = \frac{s}{V_o} = \frac{\pi/2\, R}{V_o} = \frac{\pi R}{2 V_o} \tag{38}$$

but from Eq 37

$$R = \frac{m V_o^2}{F_o} \tag{39}$$

so that Eq 38 becomes

$$t = \frac{\pi m V_o}{2 F_o} \tag{40}$$

and since $t = T$

$$T = 1{,}57 \frac{m V_o}{F_o} \tag{41}$$

The variation of the x and y components of the velocity are shown in Figure 9 also.

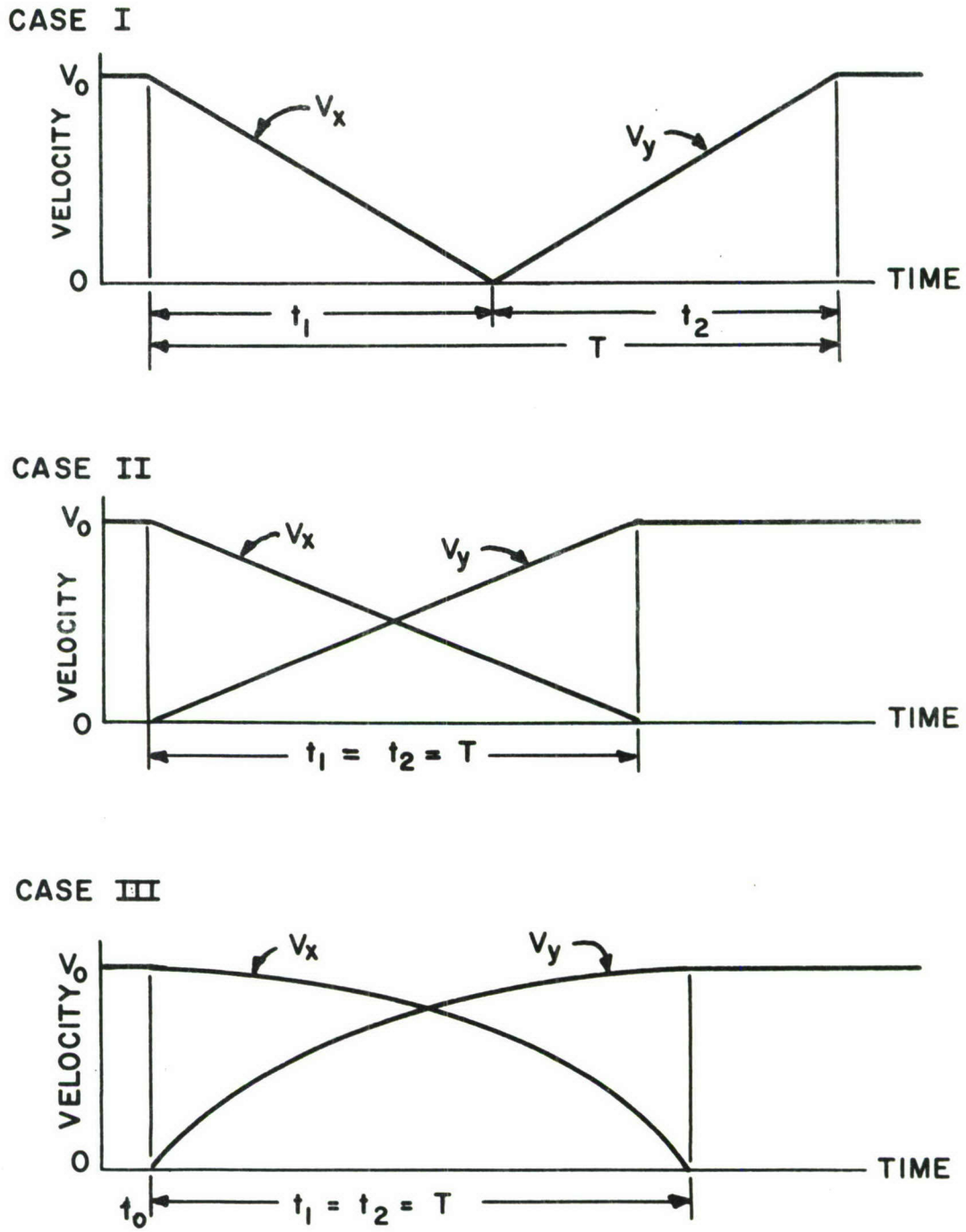

FIGURE 9

VELOCITY v.s. TIME FOR THREE TURNING MANEUVERS

Conclusions. While no attempt is made to optimize the above plane motion problem, some significant differences in maneuvering times are noted. If Case II is taken as a standard of comparison, we see that Case I takes 41.5% longer to execute the 90° turn and Case III takes 11.0% longer. In terms of fuel consumption, Case I appears to be quite impractical. It should be noted that no restriction is made on the distance required to complete the maneuver. Since this distance will vary for the three cases, any such restriction would require a reanalysis of these thrust programs.

Free-Body Dynamics

Free-floating man cannot, without some external force, affect the motion of his center of mass; but he can change his attitude by properly manipulating his appendages. Nine maneuvers have been proposed for achieving self-rotation by Kulwicki (Ref 14).

In Appendix C a more general equation of motion is derived based on conservation of angular momentum (i.e., in the absence of any external force, the total angular momentum remains constant). This derivation is based on an analysis of spacecraft docking dynamics by Grubin (Ref 10). While no particular maneuvers are described, the equation presented and the method of its development can be applied to a wide range of free-body dynamics problems.

As an example of a free-body dynamics problem, consider the free-floating space worker in an initial position with both arms raised vertically above his head. If he swings both arms (parallel to each other) forward an angle δ, his torso will be tilted backward an angle θ.

The equation for the change in body attitude (developed in Appendix C) becomes for the AF "mean man"

$$\theta = \frac{\delta}{2} - 0.86758 \arctan\left(0.86507 \tan\frac{\delta}{2}\right) \qquad (42)$$

or for each revolution of the arms, $\theta = 23.8°$.

Stability of Rotation

The moment-free motion of an unsymmetric rigid body with principal moments of inertia I_x , I_y , I_z is an unsteady periodic precession and nutation about the resultant angular momentum vector which is fixed in space. Steady rotation exists only about the principal axis of maximum or minimum moment of inertia, the principal axis of intermediate moment of inertia being unstable. Rotation about the axis of maximum or minimum moment of inertia is considered to be stable; that is, if the spin axis deviates slightly from the resultant angular momentum vector, there is no tendency for this deviation to grow. This statement can be made only for a perfectly rigid body in the absence of external moments (Ref 22).

Consider a non-rigid body rotating in space. Because of energy dissipation, the kinetic energy of rotation will decrease with time. The equation for the decrease in kinetic energy $\dot{T}$ is given by Thomson (Ref 22:214) for a body of revolution ($I_x = I_y$) with principal moments of inertia I_x, I_y, I_z to be

$$\dot{T} = I_z \omega_o^2 \left(\frac{I_z}{I_x} - 1\right)(\sin\theta\cos\theta)\dot{\theta} \qquad (43)$$

where

$\omega_o \equiv$ initial spin velocity

$\theta \equiv$ angle between the spin axis and the angular momentum vector

$\dot{\theta} \equiv$ rate at which the angle θ is changing

Since $\dot{T}$ is always negative, $\dot{\theta}$ is negative for $\frac{I_z}{I_x} > 1$ and positive for $\frac{I_z}{I_x} < 1$. If I_z is the minimum principal moment of inertia, then $\frac{I_z}{I_x}$ is less than one, $\dot{\theta}$ is positive and θ is increasing. Thus, the principal axis of minimum moment of inertia is one of unstable equilibrium, and a small deviation of the spin axis from the angular momentum vector will increase due to energy dissipation.

Man is certainly not a rigid body and under cyclic stresses induced by gyroscopic precession will dissipate energy. Hence, it can be concluded that weightless man will possess only one stable axis of rotation. This then is rotation about the principal axis of maximum moment of inertia. When it is considered that man can change this axis by moving his appendages, it is doubtful that flexible man will possess any stable axis of rotation.

Application of A Torque

The application of a torque to some relatively fixed object will be part of the function of the space worker performing assembly and repair tasks. The resulting reaction of the free-floating worker will depend upon how the torque is applied (i.e., the magnitude of the torque as it varies over a short interval of time). This reaction has been studied by Dzendolet (Ref 7); however, without exact knowledge of the nature of the torque input, and under normal 1 "g" conditions.

In this section a general equation of motion is developed and solved based on the assumption (which is experimentally validated and described in Chapter IV for a short duration, impulse-like torque) that the torque input varies as a half sine wave. Then

$$T(t) = T_M \sin \frac{\pi t}{\tau} \qquad (44)$$

where $T(t) \equiv$ torque as a function of time
$T_M \equiv$ maximum torque achieved
$\tau \equiv$ period of torque application
$t \equiv$ time

For rotation about one of the principal axes of inertia we have

$$I\dot{\omega} = T(t) = T_M \sin \frac{\pi t}{\tau} \tag{45}$$

where $I \equiv$ moment of inertia
$\dot{\omega} \equiv$ angular acceleration

Assuming I is constant, we have after integrating

$$I\omega = \frac{T_M \tau}{\pi}\left(1 - \cos \frac{\pi t}{\tau}\right) \tag{46}$$

and at $t = \tau$

$$I\omega = 2\frac{T_M \tau}{\pi} \tag{47}$$

$$\omega = 2\frac{T_M \tau}{\pi I} \tag{48}$$

Equation 48 then yields the angular velocity at the end of the torque application period.

Suppose the AF "mean man" reaches overhead to grasp a valve handle (for instance, a fuel shut-off valve on the space station). What will happen if he attempts to close the valve with a sudden twist, and the valve is frozen and does not turn?

Assume the following conditions exist:

(a) The space worker is unrestrained

(b) The torque is applied about the z-axis (a principal axis)

If the principal moment of inertia about the z-axis is

$$I_z = 0.55 \text{ slug-ft}^2$$

and the maximum torque developed is 2.71 ft.lbs over a period of 1.1 seconds, then by Eq 48

$$\omega = 0.6366 \frac{(2.71)(1.1)}{(0.55)}$$

$$= 3.45 \text{ radians/second}$$

$$= 32.9 \text{ rpm}$$

Hence, the space worker will be spinning about the z-axis at a rate of 32.9 rpm after the torque application.

IV. Experimental Results

The last phase of this study was concerned with experimental validation of some of the analytical results derived in Chapter III. Two experiments were conducted by personnel of Crew Stations Section, Behavioral Sciences Laboratory, 6570th Aerospace Medical Research Laboratories, Wright-Patterson AFB, Ohio, under weightless conditions. Zero gravity conditions were achieved for periods up to 30 seconds on-board a USAF KC-135 jet transport flying parabolic trajectories. All experiments were recorded on motion picture film.

Stability Experiment

Object. This experiment was designed to demonstrate instability of a non-rigid body rotating about the axis of minimum moment of inertia.

Procedure. The free-floating subject (holding position "a" Fig. 5 as rigidly as possible) was spun about the z-axis by means of a rope wound around the waist. Part A: The subject held position "a" throughout the free rotation period. Part B: Two to three seconds after spin-up, the subject raised one knee to induce a wobble to the spin.

Results and Discussion. Part A: Spins up to 120 rpm were achieved and appeared to be stable for the short impact-free periods (5-8 seconds).

It was intended to perform the spins so that the body z-axis was parallel to the pitch axis of the aircraft, to eliminate any cross-coupling effects due to the rotating reference system. However, there were practical difficulties in this method, and in order to get satisfactory spins and photographic coverage, it was necessary to impart the spins with the body z-axis parallel to the longitudinal axis of the

aircraft. The cross-coupling effects apparently were small as no significantly different results could be detected between the two spin axis orientations.

Part B: When one knee was flexed, a wobble in the spin did result, but the test area was not large enough to allow the subject to tumble freely without striking parts of the aircraft. Maximum impact-free periods of 5-6 seconds were not long enough to conclusively demonstrate a change to stable rotation about the x- or y-axes. A typical run is shown in Figure 10. The photographs were taken in sequence, left to right, at 0.5 second intervals.

On two of the runs the subject spread both arms and legs during the impact-free period and a decrease in rpm of 2.5 to 1 was observed.

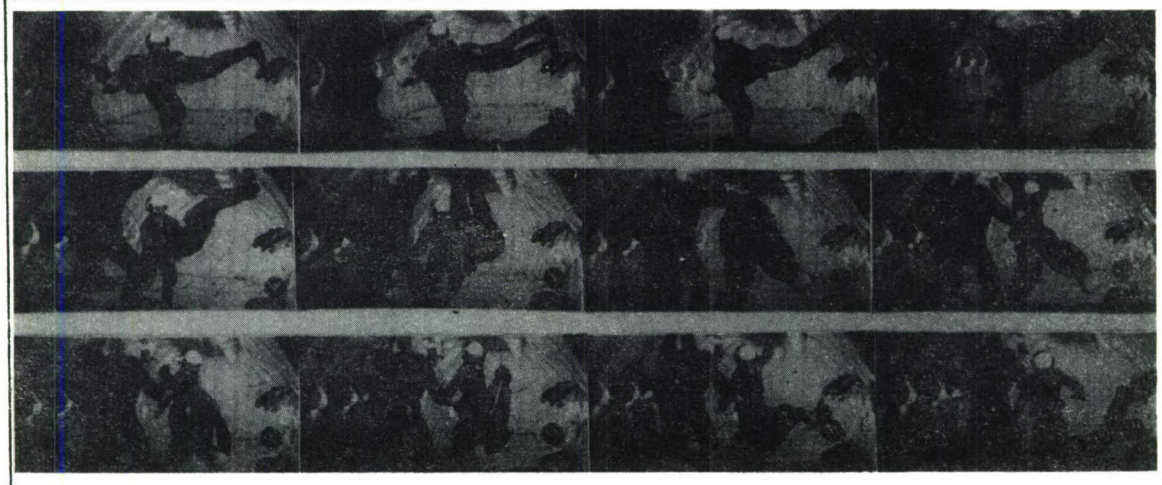

Figure 10

Sequence Photographs of the Free-Rotation of a Subject' Initially Spun About a Head-to-Toe Axis (Taken at 0.5 second intervals)

Torque Experiment

Object. This experiment was designed to determine the nature of a short duration, impulse-like torque which weightless (and hence frictionless) man can exert on a rigidly-mounted handle.

Apparatus. A small beam fitted with strain gages was attached inside a tubular handle 6 inches long and 3/4 inches in diameter. The strain gages were instrumented into the aircraft oscillograph so that strains produced deflections which were plotted as functions of time on recorder paper. The system was calibrated so that the deflections could be interpreted as torque applied to the handle.

Procedure. The weightless subject grasped the handle with his right hand and applied, with near-maximum strength, a quick counter-clock-wise torque of approximately one second duration. Part A: During the torque application and resulting rotation, the subject held body position "a" except that the right arm was extended over the head to grasp the handle. Part B: During the torque application and resulting rotation, the subject held a sitting body position (Indian fashion with legs crossed) and grasped the torque handle with the hand, arm extended, directly in front of the torso about shoulder level.

Results and Discussion. Two typical Torque vs Time plots are shown in Figure 11. As can be readily seen, these curves closely resemble a half sine wave. From Eq 48 developed in Chapter III, the resultant angular velocity can be calculated when the moment of inertia is known. The moment of inertia is found by the methods of Chapter II. These velocities are compared to actual velocities determined from motion pictures of the experiment in Table VI. The agreement is as good as can be expected when the sources of error are considered. The greatest error arises from not being able to determine the exact axis of rotation (or direction of the angular velocity vector), and hence, the moment of inertia about that axis. This error could be as large as $\pm 10\%$. Also,

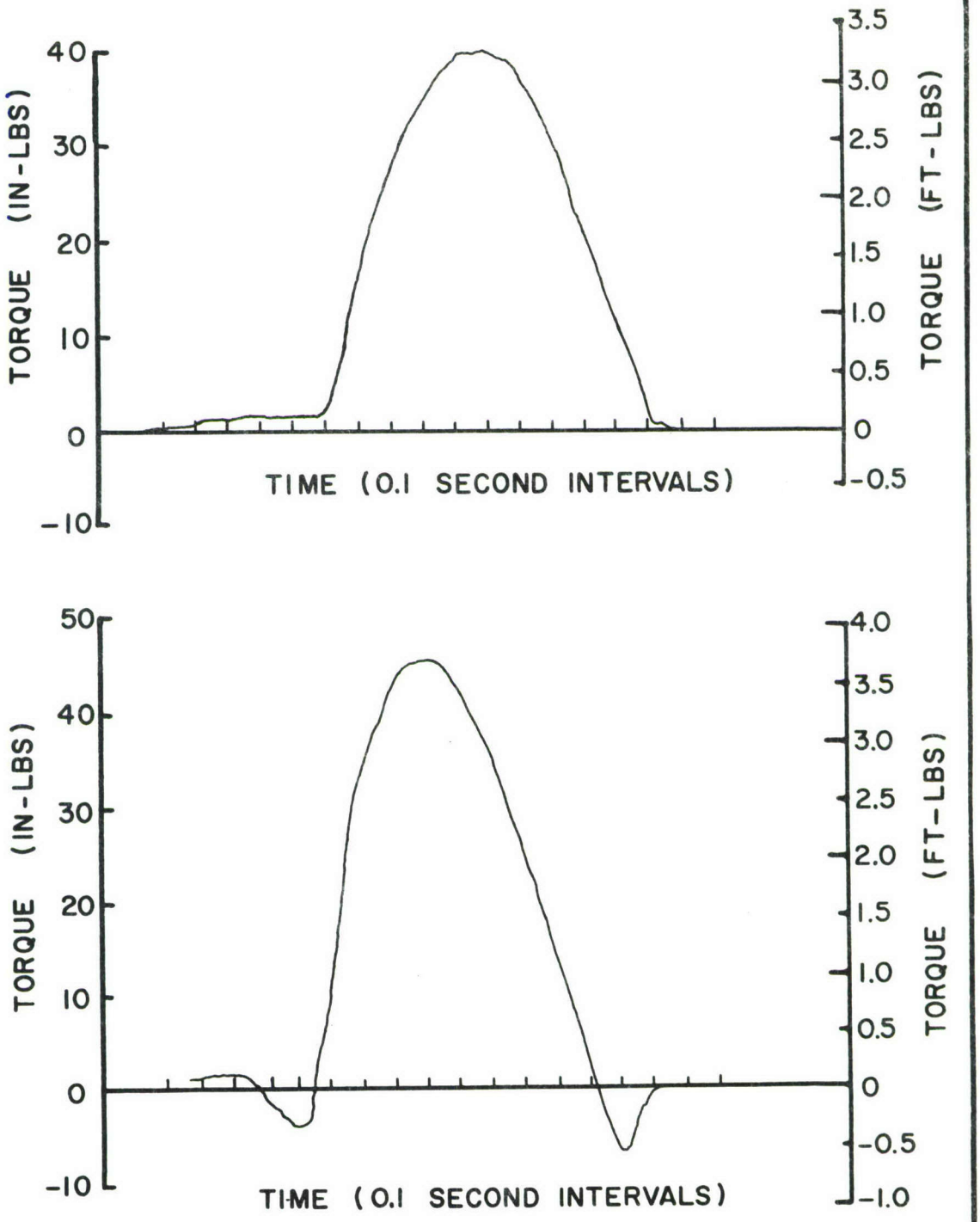

FIGURE II

TYPICAL PLOTS OF THE TORQUE THAT MAN CAN EXERT WHILE WEIGHTLESS AS A FUNCTION OF TIME

angular velocities determined by photographic means can vary ± 2%. The maximum error considering all sources should be less than ± 15%.

Table VI

Comparison of Analytical and Experimental Angular Velocities from the Torque Application Experiment

Run Number	T (seconds)	T_M (ft-lbs)	I (slug-ft^2)	ω Analytical (rad/sec)	ω Experimental (rad/sec)	Error*
2	1.10	2.71	0.55	3.45	3.59	-3.9%
5	1.00	3.34	1.05	2.02	1.86	+8.6%
6	0.88	3.75	1.05	1.99	1.86	+7.0%

*Analytical results compared to the experimental results

Conversely, the moment of inertia can be calculated from Eq 48 when the measured angular velocity is used.

The maximum torques achieved during weightlessness averaged (for six runs with two subjects) 66.6% of the peak torques under static one "g" conditions.

V. Concluding Statements and Recommendations for Future Study

The mathematical model developed to represent weightless man is based on the biomechanical properties of the human body. Since there are no methods of determining many of these properties accurately from a living subject, statistical data is used which is a function of the total body weight. Body dimensions, however, can be measured for any given living subject.

In Chapter II the transfer moment of inertia terms are shown to be a very important part of the total moment of inertia. Since the transfer term "md^2" depends upon the square of the distance between the mass and the inertia axis, it is more sensitive to variations in distance than to mass variations. Therefore, a model based on anthropometry of a given subject will reflect the dynamic response characteristics of that subject.

The statistical methods of estimating the other biomechanical properties (mass, mass center, and density) presented in References 1, 2, 4, and 6 are being refined and made more adaptable to living subjects by the Anthropology Section, Behavioral Sciences Laboratory. Hence, in the near future, methods of determining these properties from a living subject may be available.

The assumption that the human body consists of 14 rigid and homogeneous segments is a convenient, but not too realistic idealization. However, for the intended application of the model to dynamics problems facing weightless man, this assumption will not produce any great inaccuracies. For instance, first space suits will be equipped with large environmental backpacks and/or propulsion and stabilization systems

which will not allow much flexing of the back. Therefore, the assumption that the torso is rigid actually fits the physical situation.

A simplified approach is presented for calculating the new center of mass location and moments of inertia when the model's position deviates from the standing straight position (Fig 5 "a"). The resulting equations can be easily represented electrically so that the human system parameters can be programed into an analog simulator of a propulsion and stabilization system for the space maintenance worker.

The model is based on a nude man in order to establish unencumbered man's baselines (without hardware). Hardware, such as the space suit, magnetic shoes, environmental pack, etc., can be included after man's basic response characteristics have been investigated.

The analytical results are qualitative in nature and are intended to offer a first approximation to the selected problems. The simplifying assumptions are not, in general, too restrictive. For instance, the assumption that man is a body of revolution so that $I_x = I_y$ is almost satisfied for many positions (note that for position "a" $I_x = 1.046 I_y$ or I_x is 4.6% greater than I_y). Each restricted problem has practical application to the actual problems of the space worker. In summary, these problems demonstrate the requirement for a propulsion and stabilization device for the space worker.

The experimental results are preliminary in nature. However, it can be concluded that the stability experiment can not be used to verify the analytical results because of the short impact-free rotation period. The torque experiment did successfully demonstrate the practicality of the apparatus and the approach used. More data is required, however, before the analytical results can be conclusively established.

This study has been broad in scope and qualitative in the results. Hence, any one of several phases of the study might serve as a specialized thesis study area. Some suggested areas are outlined below.

Refine and validate the model: Investigate the effect of more exact representation of some of the larger segments (perhaps, use two frustums of right elliptical cones to represent the torso). Compare the moments of inertia of the model based on a particular individual to that experimentally determined for the same subject. This experimental data will become available in the near future.

Expand and generalize the dynamics problems: Investigate more problems of dynamic response to bring in the effects of muscular reaction, elasticity of the body, and damping. Generalize the selected problems of this study.

Expand the torque experiment: Conduct closely-controlled torque experiments with more subjects. Then determine the nature of the torque transmission throughout the body.

Bibliography

1. Barter, James T. Estimation of the Mass of Body Segments. WADC Technical Report 57-260. Wright-Patterson AFB, Ohio: Wright Air Development Center, April 1957. (ASTIA No. 118222)

2. Braune, W., and O. Fischer. Treatises of the Mathematical-Physical Class of the Royal Academy of Sciences of Saxony. Number 7. Leipzig, 1889. (U.S. Army Air Forces, Air Materiel Command Translation No. 379, Wright Field, Dayton, Ohio.)

3. Celentano, John T., and Harold S. Alexander. The Use of Tools in Space - An Emperical Approach. IAS Paper No. 61-145-1839. New York: Institute of the Aerospace Sciences, 1961.

4. Dempster, Wilfred Taylor. Space Requirements of the Seated Operator. WADC Technical Report 55-159. Wright-Patterson AFB, Ohio: Wright Air Development Center, July, 1955.

5. Downey, Glenn L., and Gerald M. Smith. Advanced Dynamics for Engineers. Scranton, Pennsylvania: International Textbook Company, 1960.

6. Duggar, Benjamin C. "The Center of Gravity of the Human Body." Human Factors, 4:131-148 (June 1962).

7. Dzendolet, Ernest, and John F. Rievley. Man's Ability to Apply Certain Torques While Weightless. WADC Technical Report 59-94. Wright-Patterson AFB, Ohio: Wright Air Development Center, April, 1959.

8. Grantham, William D. Effects of Mass-Loading Variations and Applied Moments on Motion and Control of a Manned Rotating Space Vehicle. NASA Technical Note D-803. Washington: National Aeronautics and Space Administration, May 1961. (ASTIA No. 255528)

9. Griffin, J. B., et al. "A Discussion of the Design of a Propulsion and Stabilization System for Man in a Cosmonotic Environment." Proceedings of the National Specialists Meeting on Guidance and Control of Aerospace Vehicles. New York: Institute of the Aerospace Sciences, 1960.

10. Grubin, Carl. Docking Dynamics for Rigid-Body Spacecraft. IAS Paper No. 62-43. New York: Institute of the Aerospace Sciences, 1962.

11. Hansen, Robert, and Douglas Y. Cornog. Annotated Bibliography of Applied Physical Anthropology in Human Engineering, edited by H. T. E. Hertzberg, WADC Technical Report 56-30. Wright-Patterson AFB, Ohio: Wright Air Development Center, May 1958.

12. Hertzberg, H. T. E., G. S. Daniels, and E. Churchill. Anthropometry of Flying Personnel-1950. WADC Technical Report 52-321. Wright-Patterson AFB, Ohio: Wright Air Development Center, September 1954.

13. Hudson, Ralph G., S. B. The Engineers' Manual (Second Edition). New York: John Wiley and Sons, Inc., 1955, pp. 89-94.

14. Kulwicki, P. V. Weightless Man: Self-Rotation Techniques, Study I. MRL TDR 62- , 6570th Aerospace Medical Research Laboratories, Aerospace Medical Division, Wright-Patterson AFB, Ohio, (in editing).

15. Petrov, V. Artificial Satellites of the Earth. Delhi, India: Hindustan Publishing Corp., 1960, p. 124.

16. Scarborough, James B. Numerical Mathematical Analysis (Fourth Edition). Baltimore: Johns Hopkins Press, 1950.

17. Seale, Leonard M., and Ralph E. Flexman. "Research on a Self-Maneuvering Unit for Orbital Workers." Proceedings of the IAS Aerospace Support and Operations Meeting. New York: Institute of the Aerospace Sciences, 1961.

18. Simons, John C., and Melvin S. Gardner. Self-Maneuvering for the Orbital Worker. WADD Technical Report 60-748. Wright-Patterson AFB, Ohio: Wright Air Development Division, December 1960.

19. Simons, John C., and W. Kama. A Review of the Effects of Weightlessness on Selected Human Motions and Sensations. A technical paper presented at the AGARD-NATO Aero Space Medical Panel Meeting, Paris, France, July 1962. Wright-Patterson AFB, Ohio: 6570th Aerospace Medical Research Laboratories, Aerospace Medical Division (AFSC), April 1962.

20. Swearingen, J. J. Determination of Centers of Gravity of Man. Final Report United States Navy Contract NAonr 104-51. Oklahoma City, Oklahoma: Civil Aeronautics Medical Research Laboratory, CAA Center, 1953.

21. Taylor, Craig L., and W. Vincent Blockley. "Crew Performance in a Space Vehicle," in Space Technology, edited by Howard S. Seifert. New York: John Wiley and Sons, 1959, p. 30-17.

22. Thomson, William Tyrrell. Introduction to Space Dynamics. New York: John Wiley and Sons, Inc., 1961.

Appendix A

Parametric Study of the Centroid Location and Moments of Inertia of a Frustum

The frustum of a right circular cone is chosen to represent the upper and lower arms and legs because its centroid can be made to coincide with the centroid of the segment it represents. The segments of the body are assumed to be bodies of revolution with known centroid locations. The location of the centroid becomes an important parameter in defining the properties of the frustum. This appendix presents a derivation of the equations for the centroid location and moments of inertia of a frustum. The equations for the moments of inertia are then expressed in much simpler form in terms of the centroid location. The mass, length, and density of the frustum are left as parameters.

Centroid of a Frustum of a Right Circular Cone

The centroid of the body shown in Figure A-1 is given by

$$\bar{y} = \frac{\int y \, dm}{\int dm} \tag{A-1}$$

where

$$dm = \delta \pi x^2 dy \tag{A-2}$$

and δ is the density (assumed to be constant at every point in the body.) Then for a frustum of length ℓ and mass m, we have

$$m = \int_0^{\ell} dm = \delta\pi \int_0^{\ell} x^2 dy \qquad \text{(A-3)}$$

for

$$x = R - \frac{(R-r)}{\ell} y \qquad \text{(A-4)}$$

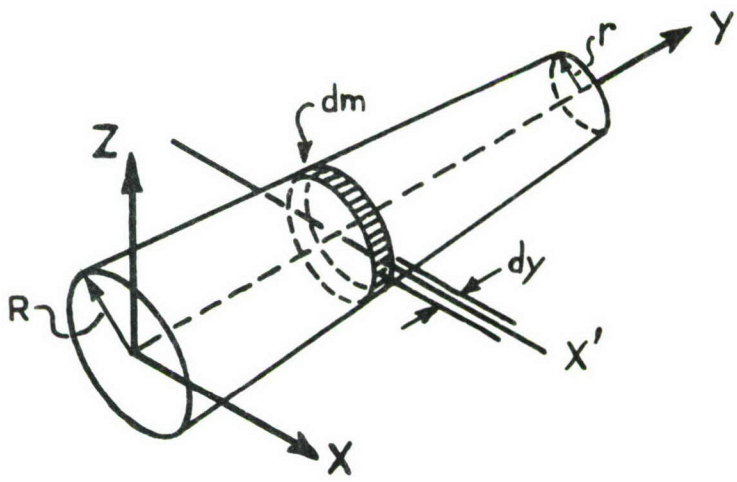

FIGURE A-1
FRUSTUM OF A RIGHT CIRCULAR CONE

Substituting Eq A-4 into Eq A-3 and integrating, we have

$$m = \frac{\delta\pi\ell}{3}\left(R^2 + Rr + r^2\right) \qquad \text{(A-5)}$$

Evaluating the numerator of Eq A-1 between the limits from 0 to ℓ, we have after substituting in Eq A-2

$$\int_0^{\ell} y\,dm = \delta\pi \int_0^{\ell} y\,x^2\,dy \tag{A-6}$$

$$= \frac{\delta\pi\ell^2}{12}\left(R^2 + 2Rr + 3r^2\right) \tag{A-7}$$

Substituting Eq A-3 and Eq A-7 into Eq A-1, Eq A-1 becomes

$$\bar{y} = \frac{\ell}{4}\left(\frac{R^2 + 2Rr + 3r^2}{R^2 + Rr + r^2}\right) \tag{A-8}$$

$$= \frac{\ell}{4}\left[\frac{1 + 2\left(\frac{r}{R}\right) + 3\left(\frac{r}{R}\right)^2}{1 + \left(\frac{r}{R}\right) + \left(\frac{r}{R}\right)^2}\right] \tag{A-9}$$

$$= \frac{\ell}{4}\left(\frac{1 + 2\mu + 3\mu^2}{1 + \mu + \mu^2}\right) \tag{A-10}$$

where

$$\mu = \frac{r}{R} \tag{A-11}$$

Introducing now the non-dimensional location at the centroid

$$n = \frac{\bar{y}}{\ell} \tag{A-12}$$

we have

$$n = \frac{1}{4}\left(\frac{1 + 2\mu + 3\mu^2}{1 + \mu + \mu^2}\right) \tag{A-13}$$

or

$$\mu = \frac{4n - 1}{1 - 2n \pm \sqrt{-12n^2 + 12n - 2}} \tag{A-14}$$

When $r = 0$ the frustum becomes a right circular cone. When $r = R$ the frustum becomes a right circular cylinder. The ratio $\frac{r}{R}$ will vary so that

$$0 \leq \mu \leq 1 \tag{A-15}$$

and

$$\frac{1}{4} \leq \eta \leq \frac{1}{2} \tag{A-16}$$

To insure that $\mu > 0$, Eq A-14 must be

$$\mu = \frac{4\eta - 1}{1 - 2\eta + \sqrt{-12\eta^2 + 12\eta - 2}} \tag{A-17}$$

Moments of Inertia of a Frustum of a Right Circular Cone

The moment of inertia about the x-axis of the element of mass shown in Figure A-1 is given by

$$I_x = \int_0^{\ell} dI_x' + \int_0^{\ell} y^2 \, dm \tag{A-18}$$

where dI_x' is the moment of inertia of the element about the x'-axis (see Fig. A-1) and dm is given by Eq A-2. Since the element of mass is a thin circular disc, its moment of inertia about an axis through its center of mass is given by

$$dI_x' = \frac{r^2 dm}{4} = \frac{\delta \pi}{4} x^4 \, dy \tag{A-19}$$

Substituting Eqs A-2 and A-19 into Eq A-18 and carrying out the integration

$$I_x = \delta\pi\int_0^{\ell}\left(\frac{x^4}{4} + x^2y^2\right)dy \tag{A-20}$$

$$= \frac{\delta\pi\ell}{20}\left(R^4 + R^3r + R^2r^2 + Rr^3 + r^4\right)$$

$$+ \frac{\delta\pi\ell^3}{30}\left(R^2 + 3Rr + 6r^2\right) \tag{A-21}$$

After some rearranging, we get

$$I_x = \frac{\delta\pi\ell\sigma R^2}{3}\left[\frac{3R^2}{20\sigma}\left(1 + \mu + \mu^2 + \mu^3 + \mu^4\right)\right.$$

$$\left. + \frac{\ell^2}{10\sigma}\left(1 + 3\mu + 6\mu^2\right)\right] \tag{A-22}$$

where

$$\sigma = 1 + \mu + \mu^2 \tag{A-23}$$

Eq A-5 can be written

$$m = \frac{\delta\pi\ell\sigma R^2}{3} \tag{A-24}$$

or

$$R^2 = \frac{3m}{\delta\pi\ell\sigma} \tag{A-25}$$

Substituting Eqs A-24 and A-25 into Eq A-22

$$I_x = m\left\{\frac{9}{20\pi}\left(\frac{1+\mu+\mu^2+\mu^3+\mu^4}{\sigma^2}\right)\left(\frac{m}{\delta\ell}\right)\right.$$

$$\left. + \frac{1}{10}\left(\frac{1+3\mu+6\mu^2}{\sigma}\right)\ell^2\right\} \qquad \text{(A-26)}$$

Letting

$$A = \frac{9}{20\pi}\left(\frac{1+\mu+\mu^2+\mu^3+\mu^4}{\sigma^2}\right) \qquad \text{(A-27)}$$

and

$$C = \frac{1}{10}\left(\frac{1+3\mu+6\mu^2}{\sigma}\right) \qquad \text{(A-28)}$$

then

$$I_x = m\left[A\left(\frac{m}{\delta\ell}\right) + C\ell^2\right] \qquad \text{(A-29)}$$

By the Parallel Axis Transfer Theorem

$$I_x = I_{x_{c.g.}} + md^2 \qquad \text{(A-30)}$$

then

$$I_{x_{c.g.}} = I_x - md^2 \qquad \text{(A-31)}$$

Substituting Eqs A-10 and A-29 into the above equation

$$I_{x_{c.g.}} = m\left[\frac{9}{20\pi}\left(\frac{1+\mu+\mu^2+\mu^3+\mu^4}{\sigma^2}\right)\frac{m}{\delta\ell}\right.$$

$$\left. + \frac{3}{80}\left(\frac{1+4\mu+10\mu^2+4\mu^3+\mu^4}{\sigma^2}\right)\ell^2\right] \qquad \text{(A-32)}$$

$$I_{x_{c.g.}} = m\left[A\cdot\left(\frac{m}{\delta\ell}\right) + B\ell^2\right] \tag{A-33}$$

where

$$B = \frac{3}{80}\left(\frac{1 + 4\mu + 10\mu^2 + 4\mu^3 + \mu^4}{\sigma^2}\right) \tag{A-34}$$

Now

$$I_y = \int_0^{\ell} dI_y' \tag{A-35}$$

where

$$dI_y' = \tfrac{1}{2} r^2\, dm \tag{A-36}$$

$$= \tfrac{1}{2}\delta\pi x^4\, dy \tag{A-37}$$

By an approach similar to that above, we get

$$I_y = \frac{2m^2}{\delta\ell} A \tag{A-38}$$

Since the frustum is a body of revolution, then

$$I_x = I_z \tag{A-39}$$

In Eqs A-29, A-33, and A-38 the quantities A, B, and C are constant for a given value of η. With the AFIT IBM 1620 Digital Computer and the assistance of Prof. R. T. Harling of the Department of Mathematics, the values of μ, A, B, and C were calculated for intervals of 0.001 over the range $0.250 \leq \eta \leq 0.500$. The results are presented graphically in Figure A-2.

The following Fortran Computer Program was used, where $R \equiv \eta, U \equiv \mu$, $S \equiv \sigma$, and H is the interval between successive values of R.

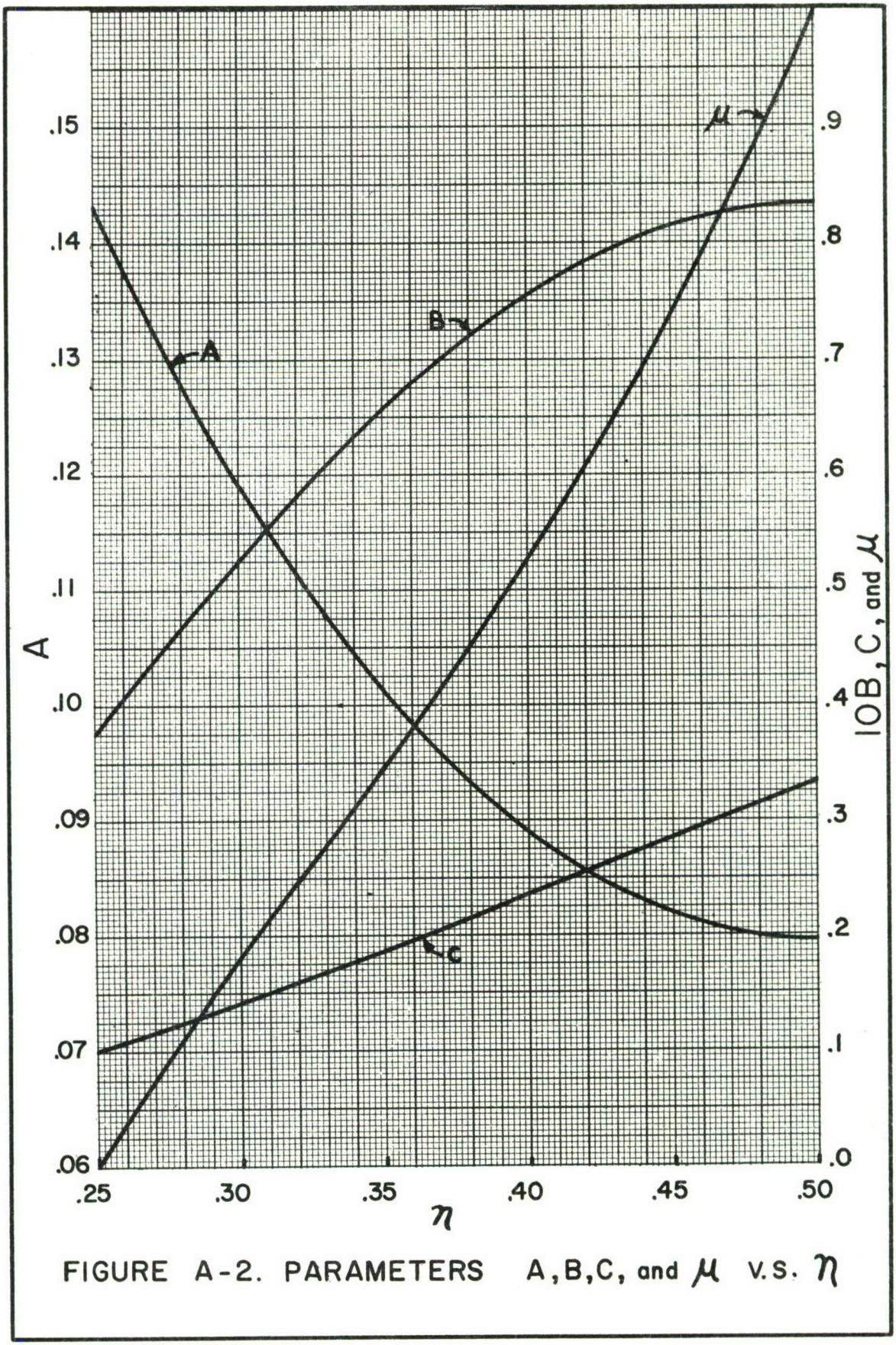

FIGURE A-2. PARAMETERS A, B, C, and μ V.S. η

```
      ACCEPT, H, RIN
      R = RIN
      PI = 3.14159265
4     U = (4.*R-1.)/(1.-2.*R+(-12.*R*R+12.*R-2.)**0.5)
      U2 = U*U
      U3 = U2*U
      U4 = U3*U
      S = 1.+U+U2
      A = ((S+U3+U4)*9.)/(20.*PI*S*S)
      B = ((1.+4.*U+10.*U2+4.*U3+U4)*3.)/(80.*S*S)
      C = ((1.+3.*U+6.*U2)*0.1)/S
      IF (SENSE SWITCH 2 ) 13, 14
13    PRINT 19,R,U,S,A,B,C
14    PUNCH 21,R,U,S,A,B,C
      R = R + H
      IF (R-0.501) 4,18,18
18    STOP
19    FORMAT (/F 5.3,F10.5,F11.5,3F10.5)
21    FORMAT (F5.3,F10.5,F11.5,3F10.5)
      END
```

Note that when $\eta = 0.250$ the frustum reduces to a right circular cone, and when $\eta = 0.500$ the frustum becomes a right circular cylinder.

This is reflected by the equations for moments of inertia. For example, when $\eta = 0.250$, $\mu = 0$, $\sigma = 1$

Eqs A-27, A-28, and A-34 yield

$$A = 0.14323 \qquad B = 0.03750 \qquad C = 0.10000$$

Then Eqs A-33 and A-39 become

$$I_{x_{c.g.}} = I_{z_{c.g.}} = m\left[0.14323\left(\frac{m}{\delta \ell}\right) + 0.03750\,\ell^2\right]$$

$$I_{y_{c.g.}} = \frac{2m^2}{\delta \ell}(0.14323)$$

Now the mass of a right circular cone is given by

$$m = \frac{\pi \delta \ell}{3} r^2 = 1.0478\ \delta \ell^2$$

so that

$$I_{x_{c.g.}} = I_{z_{c.g.}} = m\left[0.14323\left(\frac{1.0478\ \delta \ell\ r^2}{\delta \ell}\right) + 0.03750\ \ell^2\right]$$

$$= m\left(0.1500\, r^2 + 0.0375\, \ell^2\right)$$

$$= \frac{3}{20} m\left(r^2 + \frac{\ell^2}{4}\right)$$

and

$$I_{y_{c.g.}} = m\ 0.14323\left(\frac{2 \times 1.0478\ \delta \ell\, r^2}{\delta \ell}\right)$$

$$= 0.3000\, m r^2$$

$$= \frac{3}{10} m r^2$$

These are the exact equations for moments of inertia of a right circular cone.

Similarly, when $\eta = 0.500$, $\mu = 1$, $\sigma = 3$

then $A = 0.07957$ $B = 0.08333$ $C = 0.3333$

and

$$I_{x_{c.g.}} = I_{z_{c.g.}} = m\left[0.07957\left(\frac{m}{\delta \ell}\right) + 0.08333\, \ell^2\right]$$

$$I_{y_{c.g.}} = \frac{2m^2}{\delta \ell}\left(0.07957\right)$$

Now the mass of a right circular cylinder is given by

$$m = \delta \pi r^2 \ell$$

so that

$$I_{x_{c.g.}} = I_{z_{c.g.}} = m\left[0.07957\left(\frac{\delta l \pi r^2}{\delta l}\right) + 0.08333\, l^2\right]$$

$$= m\left[0.2500\, r^2 + 0.08333\, l^2\right]$$

$$= \frac{m}{12}\left[3r^2 + l^2\right]$$

and

$$I_{y_{c.g.}} = m(0.07957)\left(\frac{2 \times \delta \pi r^2 l}{\delta l}\right)$$

$$= 0.5000\, m r^2$$

$$= \frac{m r^2}{2}$$

These are the exact equations for moments of inertia of a right circular cylinder.

Sample Calculation

Find the local moments of inertia of the upper arm of the Air Force "mean man."

From Table D-I, $\eta = 0.436$

From Eqs A-14, A-27, A-34, and A-28, or Figure A-2

$\mu = 0.67445$ $\qquad$ $A = 0.08349$

$B = 0.08006$ $\qquad$ $C = 0.27016$

Eqs A-29, A-33, and A-38 become

$$I_x = I_z = m\left[0.08349\left(\frac{m}{\delta l}\right) + 0.2716\, l^2\right]$$

$$I_{x_{c.g.}} = I_{z_{c.g.}} = m\left[0.08349\left(\frac{m}{\delta l}\right) + 0.08006 l^2\right]$$

$$I_y = I_{y_{c.g.}} = 0.16698 \frac{m^2}{\delta l}$$

Also from Table D-I

$$\delta = 70.0 \text{ lbs}/\text{ft}^3$$

$$l = 13.0 \text{ in.}$$

$$m = 5.10 \text{ lbs.}$$

then the moments of inertia about the mass center are found to be

$$I_{x_{c.g.}} = I_{z_{c.g.}} = \frac{5.10}{32.2}\left[\frac{0.08349 \times 5.10}{70.0 \times \frac{13.0}{12}} + 0.08006\left(\frac{13.0}{12.0}\right)^2\right]$$

$$= 0.0157 \text{ slug-ft}^2$$

$$I_{y_{c.g.}} = \frac{0.16698\left(\frac{5.10}{32.2}\right)^2}{\left(\frac{70.0}{32.2}\right)\left(\frac{13.0}{12}\right)}$$

$$= 0.00178 \text{ slug-ft}^2$$

Appendix B

Equations of Motion for the Thrust Misalignment Problem

Symbols

x, y, z	Body Axis System Coordinates (coinciding with the principal axes)
X, Y, Z	Fixed or Inertial Axis System
$\hat{\imath}, \hat{\jmath}, \hat{k}$	Unit Vectors corresponding to the Body Axis System
$\hat{\imath}_o, \hat{\jmath}_o, \hat{k}_o$	Unit Vectors corresponding to the Inertia Axis System
I_x, I_y, I_z	Principal Mass Moments of Inertia

Conditions

The following conditions are assumed for solution of the equations of motion for the thrust misalignment problem.

1. Rigid Body
2. Constant mass "m"
3. Constant Moment about the y-y Body Axis
4. Constant Thrust "F" in the direction of the x-x Body Axis
5. $I_x = I_y$

Using a vector notation

Force Vector $$\bar{F} = F\hat{\imath} \tag{B-1}$$

Position Vector $$\bar{r} = \epsilon\hat{k} \tag{B-2}$$

Moment Vector $$\bar{M} = \bar{r} \times \bar{F} \tag{B-3}$$

$$= \epsilon\hat{k} \times F\hat{\imath} = \epsilon F\hat{\jmath} \tag{B-4}$$

But $$\bar{M} = M_x\hat{\imath} + M_y\hat{\jmath} + M_z\hat{k} \tag{B-5}$$

Therefore $$M_x = M_z = 0 \tag{B-6}$$

and $$M_y = \epsilon F \tag{B-7}$$

Then Euler's Equations

$$M_x = I_x\dot{\omega}_x + (I_z - I_y)\omega_y\omega_z \tag{B-8}$$

$$M_y = I_y\dot{\omega}_y + (I_x - I_z)\omega_x\omega_z \tag{B-9}$$

$$M_z = I_z\dot{\omega}_z + (I_y - I_x)\omega_x\omega_y \tag{B-10}$$

become

$$0 = I_x \dot{\omega}_x + (I_z - I_x)\omega_y \omega_z \tag{B-11}$$

$$\epsilon F = I_y \dot{\omega}_y + (I_x - I_z)\omega_x \omega_z \tag{B-12}$$

$$0 = I_z \dot{\omega}_z \tag{B-13}$$

From Eq B-13

$$I_z \omega_z = \text{constant} \tag{B-14}$$

If the body is initially at rest

$$\omega_z = 0 \tag{B-15}$$

and the constant is zero. Eqs B-11 and B-12 become

$$0 = I_x \dot{\omega}_x \tag{B-16}$$

$$\epsilon F = I_y \dot{\omega}_y \tag{B-17}$$

By the same reasoning applied to Eq B-13, Eq B-16 yields

$$\omega_x = 0 \tag{B-18}$$

Also Eq B-17 yields

$$\omega_y = \frac{\epsilon F}{I_y} t \tag{B-19}$$

for zero initial conditions.

Now

$$\bar{\omega} = \omega_x \hat{\imath} + \omega_y \hat{\jmath} + \omega_z \hat{k} \tag{B-20}$$

but by Eqs B-15, B-18, and B-19

$$\bar{\omega} = \omega_y \hat{\jmath} = \frac{\epsilon F}{I_y} t \, \hat{\jmath} \tag{B-21}$$

When the products of inertia are zero, angular momentum about the mass center of a rotating body is given by

$$\bar{h}_c = I_x \omega_x \hat{\imath} + I_y \omega_y \hat{\jmath} + I_z \omega_z \hat{k} \tag{B-22}$$

Substituting Eqs B-15 and B-18 into Eq B-22

$$\bar{h}_c = I_y \omega_y \hat{\jmath} = h_y \hat{\jmath} \tag{B-23}$$

hence

$$h_x = h_z = 0 \tag{B-24}$$

Now the moment about the mass center is given by

$$\bar{M}_c = \dot{\bar{h}}_c + \bar{\omega} \times \bar{h}_c \qquad \text{(B-25)}$$

After substituting and carrying out the indicated operations

$$\epsilon F \hat{\jmath} = \dot{h}_y \hat{\jmath} + \omega_y \hat{\jmath} \times h_y \hat{\jmath} \qquad \text{(B-26)}$$

$$= \dot{h}_y \hat{\jmath} \qquad \text{(B-27)}$$

Therefore, this moment increases the magnitude of the angular momentum, but does not change its direction. Hence, the angular momentum and angular velocity vectors remain parallel and fixed (in direction) in space. The only rotation is, then, a spin about the y-y body axis which also remains fixed (in direction) in space. The thrust is then applied in a plane perpendicular to the y-y axis and the resulting translation is in the same plane. If the body axis system is initially aligned with the inertial axis system, then the x-z body plane will remain in the X-Z inertial plane. The only motion between the two axis systems is translation in the X-Z inertial plane and rotation about the y-y body axis. The unit vector transformation becomes

$$\hat{\imath} = \hat{\imath}_o \cos\theta - \hat{k}_o \sin\theta \qquad \text{(B-28)}$$

$$\hat{\jmath} = \hat{\jmath}_o \qquad \text{(B-29)}$$

where θ is the angle between the z-z and Z-Z axes (or rotation between the two axis systems).

By Newton's Equation

$$\bar{F} = m \bar{a}_o \qquad \text{(B-30)}$$

$$F \hat{\imath} = m \left(a_{x_o} \hat{\imath}_o + a_{y_o} \hat{\jmath}_o + a_{z_o} \hat{k}_o \right) \qquad \text{(B-31)}$$

but $$F \hat{\imath} = \hat{\imath}_o F \cos\theta - \hat{\jmath}_o F \sin\theta \qquad \text{(B-32)}$$

or $$\hat{\imath}_o F \cos\theta - \hat{\jmath}_o F \sin\theta = m a_{x_o} \hat{\imath}_o + m a_{y_o} \hat{\jmath}_o + m a_{z_o} \hat{k}_o \qquad \text{(B-33)}$$

therefore $$F \cos\theta = m a_{x_o} \qquad \text{(B-34)}$$

$$0 = m a_{y_o} \tag{B-35}$$

$$-F \sin\theta = m a_{z_o} \tag{B-36}$$

and

$$\ddot{x}_o = \frac{F}{m} \cos\theta \tag{B-37}$$

$$\ddot{y}_o = 0 \tag{B-38}$$

$$\ddot{z}_o = -\frac{F}{m} \sin\theta \tag{B-39}$$

Now the angular velocity of the body-fixed axis system with respect to the inertial system is

$$\bar{\omega} = \dot{\theta} \hat{\jmath}_o \tag{B-40}$$

and from Eq B-21 $\frac{\epsilon F t}{I_y} \hat{\jmath} = \dot{\theta} \hat{\jmath}_o = \dot{\theta} \hat{\jmath}$ (B-41)

therefore

$$\dot{\theta} = \frac{\epsilon F t}{I_y} \tag{B-42}$$

and integrating

$$\theta = \frac{\epsilon F t^2}{2 I_y} = K t^2 \tag{B-43}$$

for $\dot{\theta} = 0$ at $t = o$, and

$$K = \frac{\epsilon F}{2 I_y} \tag{B-44}$$

Substituting for θ in Eqs B-37 and B-39 and integrating, the coordinates of the trajectory become

$$x_o = \frac{F}{m} \iint \cos K t^2 dt\, dt \tag{B-45}$$

$$y_o = 0 \tag{B-46}$$

$$z_o = -\frac{F}{m} \iint \sin K t^2 dt\, dt \tag{B-47}$$

Eqs B-45 and B-47 can be nondimensionalized by substituting

$$T^2 = K t^2 \tag{B-48}$$

$$X = \frac{mK}{F} x_o \tag{B-49}$$

$$Z = \frac{mK}{F} z_o \tag{B-50}$$

Then

$$X = \iint \cos \tau^2 d\tau d\tau \tag{B-51}$$

$$Z = -\iint \sin \tau^2 d\tau d\tau \tag{B-52}$$

Note also

$$dX/d\tau = \dot{X} = \int \cos \tau^2 d\tau \tag{B-53}$$

$$dZ/d\tau = \dot{Z} = -\int \sin \tau^2 d\tau \tag{B-54}$$

Solution

Equations B-51, B-52, B-53, and B-54 could not be integrated to get a closed form solution. However, a numerical solution was achieved by applying the Runge-Kutta Method (Ref 16:299) and computing the functions point by point on the AFIT IBM 1620 Digital Computer. The following Fortran input program was used where

T ≡ τ	H ≡ Interval between points
X ≡ X	XP ≡ dX/dτ
Z ≡ Z	ZP ≡ dZ/dτ

and the "IN" after the above symbols refers to initial conditions. The results are given graphically in Figures B-1 and B-2.

```
ACCEPT, H, TIN, XIN, XPIN, ZIN, ZPIN
T = TIN
X = XIN
Z = ZIN
XP = XPIN
ZP = ZPIN
1 PRINT, T, X, XP, Z, ZP
F1 = H * CØS(T*T)
F2 = H * CØS((T + .5 * H)** 2)
F3 = F2
F4 = H * CØS((T + H)** 2)
DELX = H * (XP + (F1 + F2 + F3)/6.)
DELXP = (F1 + 2.*(F2 + F3) + F4)/6.
X = X + DELX
XP = XP + DELXP
```

```
F1 = - H * SIN(T*T)
F2 = -H * SIN((T + .5*H)**2)
F3 = F2
F4 = -H * SIN((T + H)**2)
DELZ = H * (ZP + (F1 + F2 + F3)/6.)
DELZP = (F1 + 2.*(F2 + F3) + F4)/6.
Z = Z + DELZ
ZP = ZP + DELZP
T = T + H
GØ TØ 1
END
```

The solution is then

$$x = \eta X \tag{B-55}$$
$$z = \eta Z \tag{B-56}$$
$$\dot{x} = \eta\sqrt{k}\,\dot{X} \tag{B-57}$$
$$\dot{z} = \eta\sqrt{k}\,\dot{Z} \tag{B-58}$$
$$\theta = kt^2 \tag{B-59}$$
$$\dot{\theta} = 2kt \tag{B-60}$$

where

$$\eta = \frac{2I_y}{\epsilon m} \tag{B-61}$$

Example

The AF "mean man" is equipped with a thrust device rigidly attached to his back such that its thrust vector passes through his center of mass when he is in position "a" (Fig. 5). However, just before firing the device (capable of generating 10 lbs. of thrust), he changes to position "b". What is the resulting motion, assuming the conditions previously listed apply?

From Eq 24, Chapter II, and the tabular data in Appendix D

$$\bar{z} = \frac{\sum_{i=1}^{n} m_i\left(z_i - z_{i_0}\right)}{M}$$

$$= \Big\{2\left[1.16(14.672 + 7.406)\right] + 2\left[3.03(8.138 - 0.114)\right] + 2\left[16.33(1.355 + 11.406)\right] + 2\left[8.05(2.181 + 27.286)\right] + 2\left[2.39(-8.256 + 37.716)\right]\Big\} \div 162.22$$

$$= 6.977 \text{ in.} = \epsilon$$

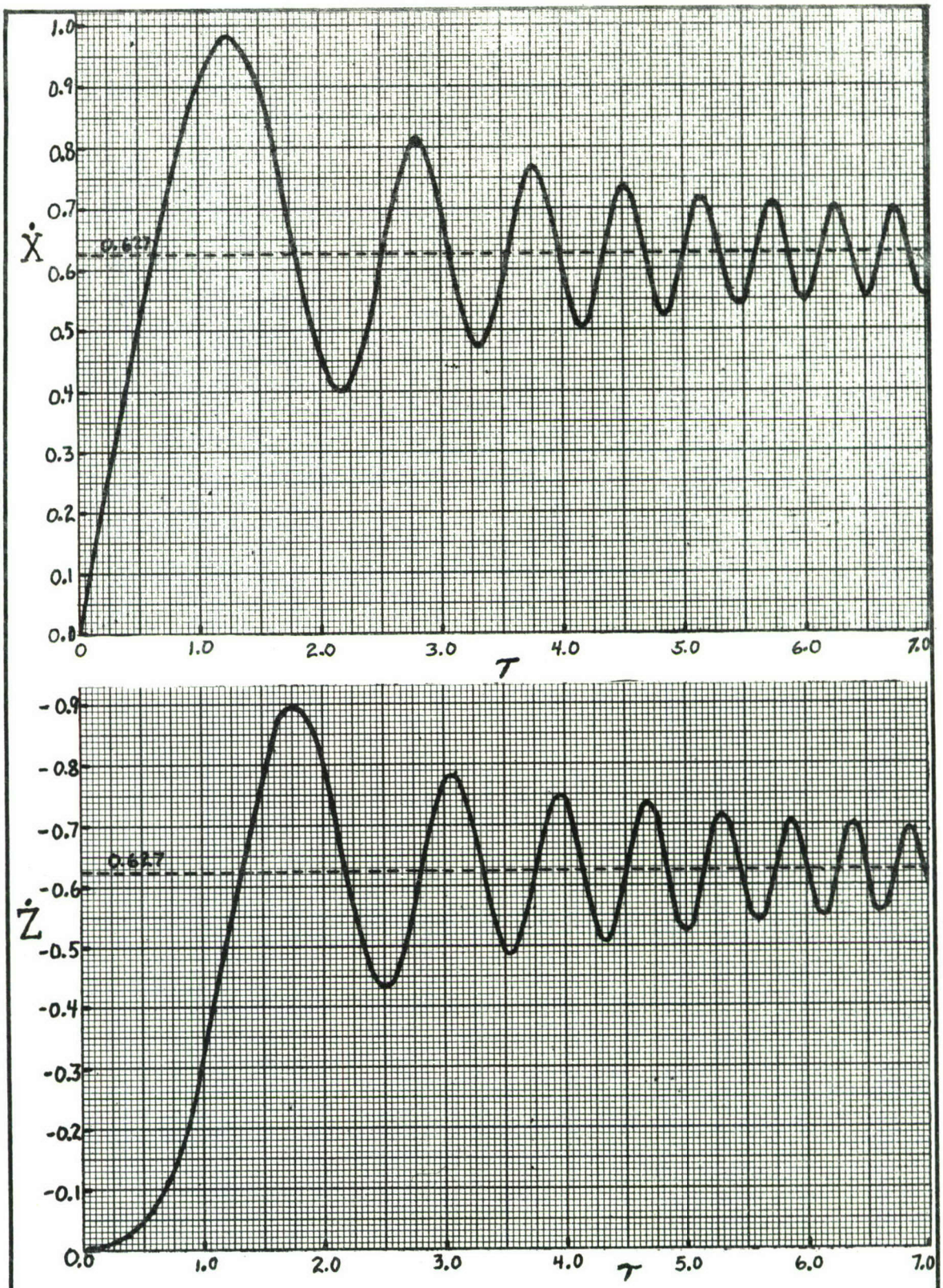

FIGURE B-1

NONDIMENSIONAL VELOCITY COMPONENTS AS A FUNCTION OF τ

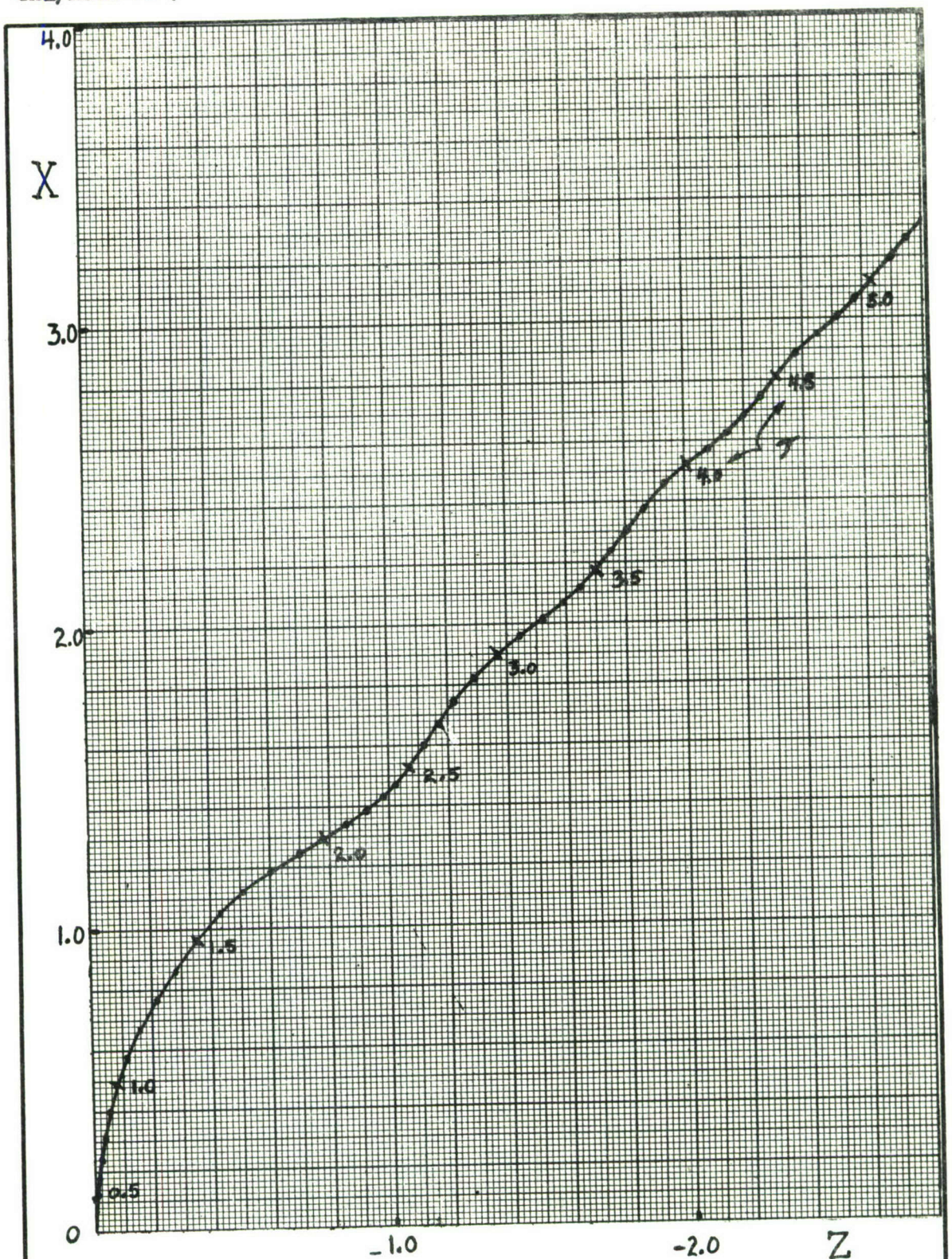

FIGURE B-2

NONDIMENSIONAL TRAJECTORY AS A FUNCTION OF τ

For the AF "mean man"

$$m = 5.0379 \text{ slugs}$$
$$I_y = 2.9445 \text{ slug-ft}^2$$

Then Eq B-44 yields

$$k = \frac{\frac{6.977}{12} \times 10}{2 \times 2.9445} = 0.9873/\text{sec}^2$$

and from Eq B-61

$$\eta = \frac{2 \times 2.9445}{\frac{6.977}{12} \times 5.0379} = 2.0105/\text{ft}$$

Eq B-48 yields

$$\tau = 0.994t$$

and Eqs B-55 through B-60 become

$$x = 2.01X \qquad \dot{x} = 2.00\dot{X}$$
$$z = 2.01Z \qquad \dot{z} = 2.00\dot{Z}$$
$$\theta = 0.987t^2 \qquad \dot{\theta} = 1.975t$$

The values of these functions are given for various times in Table B-I.

Table B-I

Numerical Results of the Misaligned Thrust Problem

t (seconds)	x (feet)	$\dot{x}$ (ft/sec)	z (feet)	$\dot{z}$ (ft/sec)	θ (degrees)	$\dot{\theta}$ (rpm)
1.008	0.160	1.900	-0.162	-0.649	57.5	19.2
2.016	2.620	0.924	-1.572	-1.610	230.0	38.3
3.022	3.830	1.411	-2.740	-1.553	516.0	57.5
5.030	6.280	1.223	-5.300	-1.056	1430.9	95.9
10.060	12.590	1.202	-11.590	-1.167	5720.0	191.4

Appendix C

Free-Body Dynamics Problem

Symbols

$\hat{e}_1, \hat{e}_2, \hat{e}_3$	Unit vectors corresponding to the x, y, z Body-Fixed Axis System at the mass center of mass m
$\hat{E}_1, \hat{E}_2, \hat{E}_3$	Unit vectors corresponding to the X, Y, Z Body-Fixed Axis System at the mass center of mass M
$\bar{P}_c, \bar{p}_c$	Position vectors from the hinge point to the individual mass centers
$\bar{\omega}$	Angular velocity of mass m
$\bar{\Omega}$	Angular velocity of mass M
$\bar{\mu}$	Net angular velocity of the system
$\bar{H}_c$	Total angular momentum of the system about the mass center
$\bar{H}$	Angular momentum of mass M
$\bar{h}$	Angular momentum of mass m
I	Moment of inertia of mass M about its mass center
i	Moment of inertia of mass m about its mass center

Derivation of Equations

The system of two rigid masses shown in Figure C-1 is hinged at point "h" so that the mass centers and point "h" remain in the same plane. Assume that initially

$$\delta = 0 \tag{C-1}$$

$$\dot{\delta} = \text{constant} = \mu_0 \tag{C-2}$$

$$\bar{H}_c = 0 \tag{C-3}$$

and there are no external forces. From Figure C-1 it can be seen that

$$\bar{P}_c = a\,\hat{E}_1 \tag{C-4}$$

$$\bar{p}_c = -b\,\hat{e}_1 = -b\cos\delta\,\hat{E}_1 - b\sin\delta\,\hat{E}_2 \tag{C-5}$$

$$\bar{\omega} = \omega\,\hat{e}_3 = \omega\,\hat{E}_3 \tag{C-6}$$

$$\bar{\Omega} = -\Omega\,\hat{E}_3 \tag{C-7}$$

$$\dot{\delta}\,\hat{e}_3 = \bar{\mu} = \mu_0\,\hat{E}_3 \tag{C-8}$$

$$\bar{H} = -I\,\Omega\,\hat{E}_3 \tag{C-9}$$

$$\bar{h} = i\omega\,\hat{e}_3 = i(\mu_0 - \Omega)\,\hat{e}_3 \tag{C-10}$$

● MASS CENTER OF EACH MASS (c.m.)

◎ MASS CENTER OF THE TOTAL SYSTEM (c.c.m.)

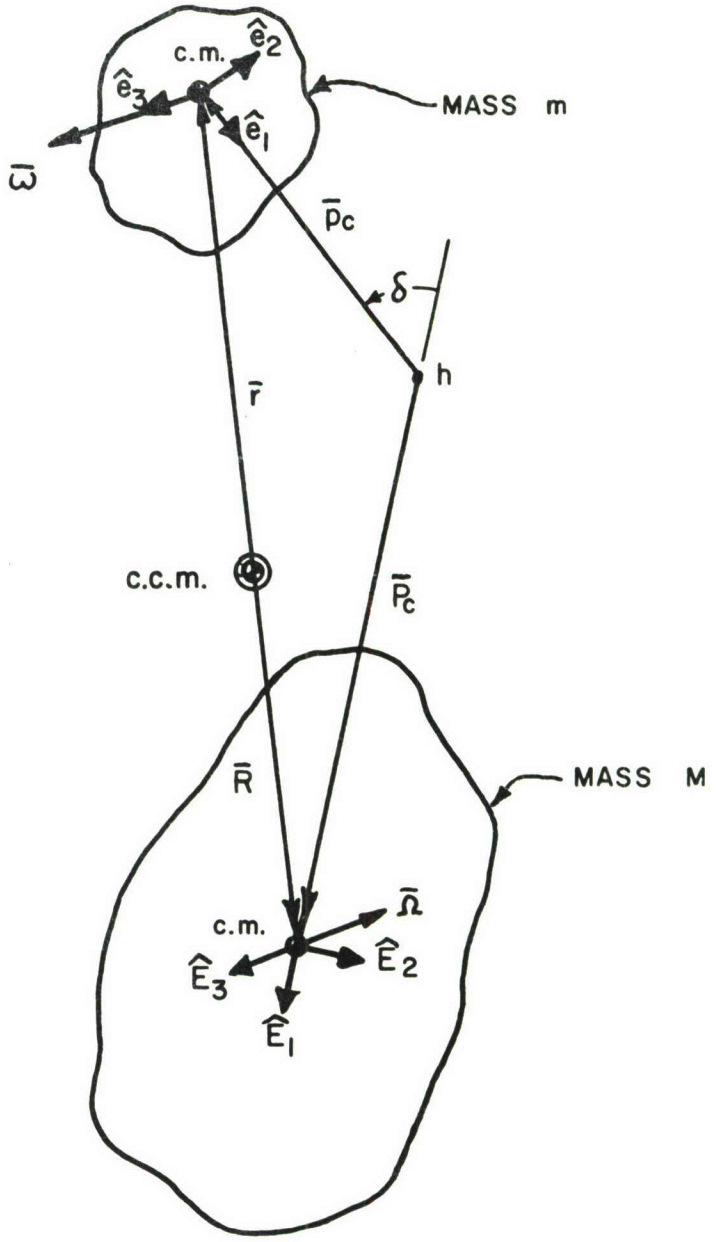

FIGURE C - 1

VECTOR DIAGRAM and BODY-FIXED AXIS SYSTEMS

Since c.c.m. is the mass center of the whole system

$$M\bar{R} + m\bar{r} = 0 \tag{C-11}$$

or

$$\bar{r} = -\frac{M}{m}\bar{R} = -\frac{1}{\epsilon}\bar{R} \tag{C-12}$$

where ϵ is the mass ratio $\frac{m}{M}$

Now define

$$\bar{R} + \bar{q} = \bar{r} \tag{C-13}$$

Solving Eqs C-12 and C-13 simultaneously

$$\bar{R} = -\bar{q}(1+\epsilon)^{-1}\epsilon \tag{C-14}$$

$$\bar{r} = \bar{q}(1+\epsilon)^{-1} \tag{C-15}$$

The total momentum of the system can be written (Ref 10)

$$\bar{H}_c = \bar{H} + M\bar{R}\times\dot{\bar{R}} + \bar{h} + m\bar{r}\times\dot{\bar{r}} \tag{C-16}$$

and by Eq C-3

$$0 = \bar{H} + M\bar{R}\times\dot{\bar{R}} + \bar{h} + m\bar{r}\times\dot{\bar{r}} \tag{C-17}$$

Substituting Eqs C-9, C-10, C-14, and C-15 into Eq C-17, then

$$-I\Omega\hat{E}_3 + M[\bar{q}(1+\epsilon)^{-1}\epsilon]\times[\dot{\bar{q}}(1+\epsilon)^{-1}\epsilon] + i(\mu_0-\Omega)\hat{E}_3 + m[\bar{q}(1+\epsilon)^{-1}]\times[\dot{\bar{q}}(1+\epsilon)^{-1}] = 0 \tag{C-18}$$

where

$$\dot{\bar{R}} = -\dot{\bar{q}}(1+\epsilon)^{-1}\epsilon \tag{C-19}$$

$$\dot{\bar{r}} = \dot{\bar{q}}(1+\epsilon) \tag{C-20}$$

Now

$$\bar{q} = \bar{p}_c - \bar{P}_c \tag{C-21}$$

$$= -(a+b\cos\delta)\hat{E}_1 + (-b\sin\delta)\hat{E}_2 \tag{C-22}$$

and

$$\dot{\bar{q}} = \dot{\bar{q}}' + \bar{\Omega}\times\bar{q} \tag{C-23}$$

Eq C-23 becomes after simplification

$$\dot{\bar{q}} = (\mu_0-\Omega)b\sin\delta\,\hat{E}_1 + [a\Omega + b(\Omega-\mu_0)\cos\delta]\hat{E}_2 \tag{C-24}$$

Substituting Eq C-24 into C-18 and carrying out the indicated operations,

Eq C-18 becomes

$$\left[(I+i)\Omega - i\mu_o\right]\hat{E}_3 = (M\epsilon^2+m)(1+\epsilon)^{-2}\left[-(a^2+b^2+2ab\cos\delta)\Omega + (b^2+ab\cos\delta)\mu_o\right]\hat{E}_3 \qquad (C\text{-}25)$$

Equating the scalar components and combining, Eq C-25 reduces to

$$\left[I+i+(a^2+b^2+2ab\cos\delta)m(1+\epsilon)^{-1}\right]\Omega = \left[i+b(b+a\cos\delta)m(1+\epsilon)^{-1}\right]\mu_o \qquad (C\text{-}26)$$

or

$$I^c(t)\,\Omega(t) = i(t)\,\mu_o \qquad (C\text{-}27)$$

where $I^c(t)$ and $i(t)$ are instantaneous moments of inertia and

$$I^c(t) = I + i + (a^2+b^2+2ab\cos\delta)m(1+\epsilon)^{-1} \qquad (C\text{-}28)$$

$$i(t) = i + b(b+a\cos\delta)m(1+\epsilon)^{-1} \qquad (C\text{-}29)$$

Let

$$\Omega(t) = \frac{d\theta}{dt} = \dot{\theta} \qquad (C\text{-}30)$$

then

$$d\theta = \frac{i(t)}{I^c(t)}\mu_o\,dt \qquad (C\text{-}31)$$

Now

$$\delta = \mu_o t \qquad (C\text{-}32)$$

or

$$d\delta = \mu_o\,dt \qquad (C\text{-}33)$$

Substituting Eq C-33 in Eq C-31 and integrating

$$\int_0^{\theta} d\theta = \int_0^{\delta} \frac{i(t)}{I^c(t)}\,d\delta \qquad (C\text{-}34)$$

Equations C-28 and C-29 can be written

$$I^c(t) = C + D\cos\delta \qquad (C\text{-}35)$$

$$i(t) = A + B\cos\delta \qquad (C\text{-}36)$$

where $$A = i + b^2 m (1+\epsilon)^{-1} \quad (C-37)$$

$$B = abm (1+\epsilon)^{-1} \quad (C-38)$$

$$C = I + i + (a^2+b^2) m (1+\epsilon)^{-1} \quad (C-39)$$

$$D = 2abm (1+\epsilon)^{-1} \quad (C-40)$$

and are constant for a given problem. Equation C-34 then becomes

$$\theta = \int_0^{\delta} \frac{A + B\cos\delta}{C + D\cos\delta}\, d\delta \quad (C-41)$$

Integrating the right hand side of Eq C-41

$$\theta = \frac{\delta}{2} + \frac{(2A-C)}{\sqrt{C^2-D^2}} \arctan\left(\frac{\sqrt{C^2-D^2}}{C+D} \tan\frac{\delta}{2} \right) \quad (C-42)$$

$$\theta = \frac{\delta}{2} + \frac{I_2}{I_1} \arctan\left(\frac{I_1 \tan\frac{\delta}{2}}{I'(0)} \right) \quad (C-43)$$

where

$$I_1 = \sqrt{C^2-D^2} = \left[(I+i)^2 + 2m(I+i)(a^2+b^2)(1+\epsilon)^{-1} + m^2(a^2-b^2)^2(1+\epsilon)^{-2} \right]^{1/2} \quad (C-44)$$

$$I_2 = 2A - C = i - I + m(1+\epsilon)^{-1}(b^2-a^2) \quad (C-45)$$

$$I'(0) = C + D = I'(t)\big|_{at\ t=0} \quad (C-46)$$

$$= i + I + (a^2+b^2) m (1+\epsilon)^{-1} + 2abm(1+\epsilon)^{-1} \quad (C-47)$$

Hence, the change in the attitude of the large mass "M" is a function of the rotation δ of the small mass "m".

Example

If the small mass "m" represents both arms (including the hands) of the AF "mean man," and "M" represents the total mass less that of "m", Eq C-43 can be used to calculate the change in body attitude when the arms are rotated. Then, from the tabular data in Appendix D, and the above equations

$a = 1.511$ ft
$b = 0.988$ ft
$\epsilon = 0.1294$
$\lambda = 0.2508$ slug-ft^2
$I = 8.6811$ slug-ft^2
$I_1 = 10.4866$ slug-ft^2
$I_2 = -9.0980$ slug-ft^2
$I^*(o) = 12.1223$ slug-ft^2

and

$$\theta = \frac{\delta}{2} - 0.8676 \arctan (0.86507 \tan \frac{\delta}{2})$$

for $\delta = 360^\circ$

$$\theta = 180^\circ - 0.8676 (180^\circ)$$

$$= 23.84^\circ$$

Appendix D

TABULAR DATA

Table D-I
Biomechanical Properties of the Segments
of the AF "Mean Man"

Segment	Weight (pounds)	Density (lbs/ft)	Length (inches)	Centroid Location (% length)
Head	11.20	71.6	10.04[a]	50.0
Torso	78.90	68.6	24.56[a]	50.0
Upper Arm	5.10[c]	70.0	13.00[a]	43.6[b]
Lower Arm	3.03[c]	70.0	10.00[a]	43.0[b]
Hand	1.16[c]	71.7	3.69	50.0
Upper Leg	16.33[c]	68.6	15.80[a]	43.3[b]
Lower Leg	8.05[c]	68.6	15.99[a]	43.3[b]
Foot	2.39[c]	68.6	2.73[a]	50.0

a - Ref 12 b - Ref 4
c - Mr. C. E. Clauser, Anthropology Section, Aero-Med Research Laboratories

Table D-II
Coordinates of the Segment Hinge Points and Mass Centers

Hinge Point and Symbol*	Coordinates (Inches)		
	X	Y	Z
Neck • A	0	0	59.08
Shoulder • B	0	7.88	56.50
Elbow • C	0	7.88	43.50
Hip • D	0	3.30	34.52
Knee • E	0	3.30	18.72
Mass Center and Symbol*			
Head ⊙ 1	0	0	64.10
Torso ⊙ 2	0	0	46.80
Upper Arm ⊙ 3	0	7.88	50.83
Lower Arm ⊙ 4	0	7.88	39.20
Hand ⊙ 5	0	7.88	31.68
Upper Leg ⊙ 6	0	3.30	27.68
Lower Leg ⊙ 7	0	3.30	11.80
Foot ⊙ 8	2.45	3.30	1.37

*Symbols Indicated in Figure 2

Table D-III
(To be continued)
Moments of Inertia of the Segments
for Two Positions*

		Segments#			
		Head	Torso	Upper Arms	Lower Arms
$I_{x_{c.g.}}$	Position a	0.0183	1.0000	0.0157	0.0056
	Position b	0.0183	1.0000	0.0157	0.0044
md^2	Position a	1.5114	1.0125	0.2199	0.0405
	Position b	0.7859	0.0092	0.0932	0.0407
I_x	Position a	1.5297	2.0125	0.2356	0.0461
	Position b	0.8042	1.0092	0.1089	0.0451
$I_{y_{c.g.}}$	Position a	0.0183	0.9300	0.0157	0.0056
	Position b	0.0183	0.9300	0.0157	0.0056
md^2	Position a	1.5114	1.0125	0.1517	0.0000
	Position b	0.7950	0.0734	0.0292	0.0002
I_y	Position a	1.5297	1.9425	0.1674	0.0056
	Position b	0.8133	1.0034	0.0449	0.0058
$I_{z_{c.g.}}$	Position a	0.0124	0.2300	0.0018	0.0008
	Position b	0.0124	0.2300	0.0018	0.0020
md^2	Position a	0.0000	0.0001	0.0682	0.0405
	Position b	0.0091	0.0642	0.0723	0.0405
I_z	Position a	0.0124	0.2301	0.0700	0.0413
	Position b	0.0215	0.2942	0.0742	0.0426

* Positions "a" and "b" are shown in Figure 5
\# All values are in Slug-ft^2

Table D-III
(Continued)
Moments of Inertia of the Segments
for Two Positions*

		Segments				
		Hands	Upper Legs	Lower Legs	Feet	Total
$I_{x_{c.g.}}$	Position a	0.0004	0.0776	0.0372	0.0006	1.2927
	Position b	0.0004	0.0620	0.0372	0.0006	1.2589
md^2	Position a	0.0292	0.4964	1.3114	0.7388	8.1963
	Position b	0.0303	0.1496	0.0588	0.1252	1.7907
I_x	Position a	0.0296	0.5740	1.3486	0.7394	9.4890
	Position b	0.0307	0.2116	0.0960	0.1258	3.0496
$I_{y_{c.g.}}$	Position a	0.0004	0.0776	0.0372	0.0028	1.2269
	Position b	0.0004	0.0776	0.0372	0.0028	1.2269
md^2	Position a	0.0137	0.4582	1.2925	0.7361	7.8284
	Position b	0.0188	0.1190	0.1015	0.1560	1.7176
I_y	Position a	0.0141	0.5358	1.3297	0.7389	9.0553
	Position b	0.0192	0.1966	0.1387	0.1588	2.9445
$I_{z_{c.g.}}$	Position a	0.0004	0.0154	0.0037	0.0028	0.2922
	Position b	0.0004	0.0310	0.0037	0.0028	0.3258
md^2	Position a	0.0155	0.0382	0.0188	0.0085	0.3797
	Position b	0.0195	0.0459	0.0804	0.0420	0.6746
I_z	Position a	0.0159	0.0536	0.0226	0.0113	0.6719
	Position b	0.0199	0.0769	0.0841	0.0448	1.0004

* Positions "a" and "b" are shown in Figure 5, and all values are in Slug-ft^2